Journal Pre-proof

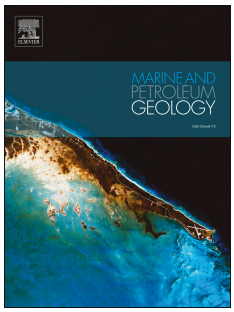

Multiple episodes of sand injection leading to accumulation and leakage of hydrocarbons along the San Andreas/San Gregorio fault system, California

Giuseppe Palladino, Roberto Emanuele Rizzo, Gustavo Zvirtes, Antonio Grippa, Ruy Paulo Philipp, David Healy, G. Ian Alsop

PII: S0264-8172(20)30214-2

DOI: https://doi.org/10.1016/j.marpetgeo.2020.104431

Reference: JMPG 104431

To appear in: *Marine and Petroleum Geology*

Received Date: 8 March 2019

Revised Date: 16 April 2020

Accepted Date: 29 April 2020

Please cite this article as: Palladino, G., Rizzo, R.E., Zvirtes, G., Grippa, A., Philipp, R.P., Healy, D., Alsop, G.I., Multiple episodes of sand injection leading to accumulation and leakage of hydrocarbons along the San Andreas/San Gregorio fault system, California, *Marine and Petroleum Geology* (2020), doi: https://doi.org/10.1016/j.marpetgeo.2020.104431.

Dear Editor,

please find enclosed the Credit Author Statement for the paper titled: Multiple episodes of sand injection leading to accumulation and leakage of hydrocarbons along the San Andreas/San Gregorio fault system, California. By Palladino et el., that we we have now finished to revise.

Palladino Giuseppe: Conceptualization, Field work, Data curation, Original draft preparation, Software.

Roberto Emanuele Rizzo: Conceptualization, Field work, Data curation, Original draft preparation, Software.

Gustavo Zvirtes: Conceptualization, Field work, Data curation, Original draft preparation, Software.

Antonio Grippa: Field work.

Ruy Paulo Philipp: Field work, Data curation.

David Healy: Reviewing and Editing, Supervision.

G. Ian Alsop: Data curation, Writing- Reviewing and Editing, Supervision.

Best wishes

Giuseppe Palladino

Multiple episodes of sand injection leading to accumulation and leakage of hydrocarbons along the San Andreas/San Gregorio fault system, California.

Giuseppe Palladino[1,2*], Roberto Emanuele Rizzo[1], Gustavo Zvirtes[1], Antonio Grippa[1], Ruy Paulo Philipp[3], David Healy[1] and G. Ian Alsop[1]

[1]Department of Geology and Geophysics, School of Geosciences, University of Aberdeen, Aberdeen, UK

[2]Dipartimento di Scienze, Università degli Studi della Basilicata, Potenza, Italy

[3]Departamento de Mineralogia e Petrologia, Universidade Federal do Rio Grande do Sul, Porto Alegre, Rio Grande do Sul, Brazil

*Corresponding author: Giuseppe Palladino, E-mail: giuseppe.palladino@abdn.ac.uk

Abstract

The presence of sand injections has been shown to enhance the likelihood of hydrocarbon traps within siliciclastic successions. Through the development of large interconnected networks of sills and dykes, sand injection complexes provide a volume of porous and permeable rocks within the low permeability host units. Overall, the formation of sand injection complexes requires extensive fracturing and hydrofracturing, which can be particularly pronounced when sand injections are coupled with brittle tectonic deformation. In some circumstances, this process may threaten the integrity of the reservoir top seal thereby preventing further hydrocarbon accumulation. Studying exceptional exposures along the coastal area of Santa Cruz in California, we report evidence for top seal failure associated with injection episodes. Two distinct sand injection episodes are proposed. The first event, datable to the Late Miocene, resulted in large volumes of sand being emplaced within the top-seal units, and was followed by accumulation of hydrocarbons within the

newly injected sandstones. Later, a series of brittle tectonic events, associated with the San Andreas/San Gregorio Fault System, caused remobilisation and accumulation of sand along newly formed fault planes. Our case study documents this combination of pervasive brittle deformation and sandstone injection along fault structures, which can ultimately disrupt the integrity of a host unit leading top seal failure and leakage of hydrocarbons.

Keywords: Sandstone intrusions; Santa Cruz Injection Complex; Santa Cruz petroleum system; Sandstone-filled faults; Hydrocarbon leakage; San Andreas/San Gregorio fault system; California.

1. Introduction

Emplacement of sandstone intrusions in the shallow crust is frequently associated with fracturing and faulting processes that are caused either by an excess of pore-fluid pressure, or by regional tectonic stresses. The injection of sandstone intrusions has been proposed as a potential mechanism capable of generating top seal failure in sedimentary successions where sands alternate with low-permeability mudstones (Molyneux et al., 2002; Hurst et al., 2003; Cartwright et al., 2007). Hydrofracturing and faulting processes linked to fluid overpressure commonly initiate at the interface between the reservoir rocks and top seal strata, when fluid pressure exceeds the fracture gradient and then propagates throughout the top seal sequence (Jolly and Lonergan, 2002). Fractures and faults related to regional tectonic stresses also commonly involve, and cut through, the interface between the reservoir/top seal system (Palladino et al., 2018).

In general, fracture processes affecting poorly-consolidated top seal sediments result in a momentary failure of the system, which is immediately followed by fracture resealing similar to the mechanism described by Sibson (1990). At the end of this process, sandstone intrusions will provide additional porosity and permeability to the system, with associated positive repercussions for oil accumulation. However, fracture processes involving well-cemented sediments can lead to either the partial or complete breaching of the sealing sequence, with two contrasting outcomes for

oil retention: i) partial top seal breaching generally resulting in enhanced reservoir capacity, as fault and fracture apertures, together with highly-permeable sandstone intrusions, provide new capacity for hydrocarbon accumulation; ii) alternatively, complete breaching of the sealing sequence thereby preventing hydrocarbon accumulation due to bypass mechanisms or, in the case where hydrocarbons have already accumulated in the reservoir, will result in leakage phenomena (Cartwright et al., 2007).

Given the potential importance of the above relationships, the study of the interactions between faults, fractures and sandstone intrusions cannot be ignored when exploring for hydrocarbon reserves. In this work, we present direct field evidence for top seal failure associated with emplacement of sandstone intrusions forming the Santa Cruz Injection Complex (SCIC) in the coastal area of California (Thompson et al., 2007) (Fig. 1). The SCIC shares many of its main elements with other sand injection complexes in California (e.g. Vigorito and Hurst, 2010; Scott et al., 2013) and displays a complete suite of components which comprise a source rock, an intrusive network, and an extrudite complex (Scott et al., 2009). The host rock is represented by the Santa Cruz Mudstone. The SCIC is part of the Santa Cruz petroleum system, thereby representing an ideal analogue for hydrocarbon-bearing sand injections in the subsurface (Dixon et al., 1995; Duranti et al., 2002; Duranti and Hurst, 2004).

The first studies describing sand injections in the Santa Cruz area, date back to the beginning of the 20th century (Eldridge, 1901; Newsom, 1903) and focused on the potential of mining these tar-sand deposits. After tar production decreased, successive studies focussed on the mechanisms leading to the emplacement of sandstone intrusions, and on the relationships between sand injections and tectonic structures in the area (Phillips, 1990; Molyneux, 1999; Boehm and Moore, 2002; Jolly and Lonergan, 2002; Thompson et al., 2007; Scott et al., 2009; Sherry et al., 2012). Based on contradictory field evidence, which indicates the contemporaneous occurrence of sandstone intrusions emplaced along faults, and sandstone intrusions overprinted by tectonic structures, two main mechanisms invoking episodes of pore-fluid overpressure, and tectonic processes were formulated. It is important to note that in both cases, the resulting models considered that the SCIC was emplaced as a single event. More recently Palladino et al. (2018)

showed that two different injection phases, displaying clear cross-cutting relationships, affected the SCIC.

In this study we have undertaken a detailed geological survey along the coastal sector between Santa Cruz and Davenport (Fig. 1) which allowed us to relate the two previously recognized injection stages with the whole evolution of the Santa Cruz petroleum system. In particular, our results indicate that the first injection stage occurred when the Santa Cruz Mudstone was still poorly consolidated, whereas the second stage occurred after the cementation of the top seal sediments. These conclusions allow us to propose an evolutionary model incorporating the initiation, development and the successive failure of the Santa Cruz petroleum system.

2. Geological setting

2.1 Geology of the Santa Cruz coastal area

The coastal sector between the City of Santa Cruz and Davenport is part of the "Ben Lomond domain" (*sensu* Aydin and Page, 1984), which is a relatively undeformed area between the two major San Andreas and San Gregorio dextral strike-slip fault zones (Dickinson et al., 2005) (Fig. 1a-c). The outcrops consist of a Middle Miocene-Pliocene sedimentary succession unconformably overlying the granitic/metamorphic Salinian basement, which forms the southwest flank of the Ben Lomond Mountain (Clark, 1981; Page et al., 1998) (Fig. 1d). The base of the sedimentary succession consists of shallow-marine arkosic sandstone of the Middle Miocene Lompico Formation, which rests uncomformably upon the crystalline basement. This formation reaches a maximum thickness of about 240m and is conformably overlain by bathyal biosiliceous mudrocks and sandstones of the Monterey Formation (Clark, 1981). The Monterey Formation reaches a thickness of 800m in the study area and is unconformably overlain by the Santa Margarita Sandstone (Fig. 1d). This formation consists of coarse-grained, large-scale cross-bedded arkosic sandstones and fine-grained bioturbated sandstones, deposited in a tidal/nearshore depositional environment. The unit has a maximum thickness of 130m and the coarse-grained facies contain accumulations of oil and tar. The Santa Margarita Sandstone is

considered to be the reservoir unit of the Santa Cruz petroleum system, whereas the Monterey Formation represents the source rock (see the next section). The Santa Cruz Mudstone stratigraphically overlies the Santa Margarita Sandstone (Fig. 1d), and consists of organic-rich, thickly bedded, biosiliceous mudstone and thin porcelanite layers containing dolomite and calcite concretions. Green mudstone horizons up to 10 cm thick locally alternate with the previously described mudstone lithologies. The Santa Cruz Mudstone was deposited in a shelf environment approximately 9.0–7.0 Ma ago (Barron, 1986) and reaches a maximum thickness of 2700m. It is considered to be the top seal for the Santa Cruz petroleum system. The Purisima Formation is the youngest unit recognised in the Santa Cruz area. It consists of Miocene to Pliocene, very thick-bedded tuffaceous and diatomaceous siltstones alternating with thick-bedded andesitic sandstones, deposited in a neritic environment which in places reaches 300m in thickness.

The Santa Cruz succession forms the southwestern flank of the of the Ben Lomond mountain fold (Stanley and McCaffrey, 1983) which is a southeast-plunging anticline formed between the San Andreas and San Gregorio fault zones (Fig. 1b). The succession is also affected by a series of minor NE-SW and N-S trending open anticlinal and synclinal folds (Phillips, 1990) (Fig. 1c). Other important tectonic structures in the area are the Ben Lomond and Zayante fault zones (Clark and Rietman, 1973, Clark, 1981, Brabb, 1989) (Fig. 1b).

Displacement across the Pacific-North America transform margin has been slightly compressive since 8 Ma (Atwater and Stock, 1998), resulting in a progressive tectonic uplift of the area marked by folding and faulting. In particular, a series of NW-SE trending anticlines and synclines formed between the Zayante/Ben Lomond fault system and the San Andreas Fault whereas, west of the Ben Lomond fault, a gently SW-dipping homocline forms the major structure in the study area. Uplift in the Santa Cruz area has been continuous between the late Neogene and Quaternary, with a calculated uplift rate of 0.16 m/1,000 yr (Bradley and Griggs, 1976). More recently Bürgmann et al. (1994) suggested an average uplift rate of the order of 0.8 mm/yr over the last 4.6 m.y. The SCIC is currently exposed along wave-cut platforms and cliffs in the Santa Cruz Mudstone, located on the southwestern side of Ben Lomond Mountain.

2.2. The Santa Cruz petroleum system

The Santa Cruz petroleum system (SCPS) is a fossil petroleum system that displays a complete sequence of source rock, reservoir, top seal, and overburden represented by the Monterey, Santa Margarita Sandstone, Santa Cruz Mudstone and Purisima formations, respectively (Phillips, 1990; Hosford Scheirer et al., 2013) (Fig. 1d). Petroleum generation occurred during a narrow span of time between 7Ma and 5Ma (Hosford Scheirer et al., 2013). Although the Monterey Formation is interpreted to be the source rock for the SCPS, geochemical studies suggest that the Santa Cruz Mudstone is another possible petroleum source (Lillis and Stanley, 1999). SCPS mainly consists of tar-saturated sandstones, with oil and gas recognised in the Santa Cruz Mountain area, and also along the coast. Hydrocarbons represented by both oil and gas are also present offshore along the Santa Cruz continental margin (Mullins and Nagel, 1982; Heck et al., 1990). In the coastal area, the reservoir rocks mainly consist of heavy oil and tar-saturated sandstones irregularly distributed in an area of about 120 km^2 included between Davenport, Bonny Doon and Santa Cruz (Fig. 1). Tar-saturated sandstones and hydrocarbon seeps occurring in the Santa Cruz coastal area are well-known since the end of the 19th century (Eldridge, 1901; Newsom, 1903; Jenkins, 1930), and attained moderate economic significance following the 1906 earthquake in San Francisco when sand from the Santa Margarita Sandstone was mined to provide asphalt for road rebuilding. In the same area, the occurrence of petroleum has also been ascertained and estimates of oil reserves varied from 10 million bbl to 20 million bbl which classifies the SCPS as a minor oil field (Page and Holmes, 1945; Phizackerley and Scott, 1978; Hallmark, 1980). Although the Santa Cruz petroleum system has only limited economic relevance, the significance of its study lies in the fact that it represents a valid analogue for larger subsurface oil fields.

3. The Santa Cruz Injection Complex

3.1 Factors controlling emplacement, geometry and architectural organization of sandstone intrusions

Sandstone intrusions generally originate by the forceful emplacement of fluidised sand into an actively propagating hydraulic fracture system within low permeability host rocks, although examples in high-permeability cohesionless systems have also been documented (Ross et al., 2014 and references therein). Pore-fluid pressure must exceed the fracture toughness of the host strata. Additionally, to mobilise sand from unconsolidated parent depositional units, the velocity of the pore-fluid must exceed the minimum fluidisation velocity (Lowe, 1975). For fine- to medium grained sand, the minimum fluidisation velocity is estimated to range between 0.001 ms^{-1} and 0.01 ms^{-1}, although during large-scale injection much higher velocity is inferred (Duranti and Hurst, 2004; Hurst et al., 2011, Ross et al., 2014). Pore-fluid is generally driven upward following the pressure gradients that form between high-pressured zones in the shallow crust, typically at depths of less than 1.5 km burial and the Earth's surface (Vigorito and Hurst, 2010; Hurst et al., 2011).

Variations in pore-fluid pressure within the host strata and the underlying pressure cell typically form sandstone intrusion complexes that consist of four main architectural elements comprising the parent units, dikes, sills and extrudites (Vigorito and Hurst, 2010) (Fig. 2a). The distribution and geometry of sandstone intrusions in the crust are generally the result of the interaction between pore-fluid pressure and the lithostatic pressure (overburden). For example, sills mainly develop at a depth where the fluid pressure is equal or greater than the lithostatic pressure (lithostatic equilibrium surface, LES of Vigorito and Hurst, 2010) forming a sill zone in which the greatest volume of injected sand occurs (Fig. 2a). Dikes dominate immediately above the parent units (the lower dike zone) and between the sill zone and the sand extrudites (upper dike zone) (Fig. 2a). Unlike other sandstone intrusion complexes occurring in central California (i.e. the Panoche Giant Injection Complex of Vigorito and Hurst, 2010), the SCIC displays rare vertical and lateral relationships due to tectonic disturbance. However, the different architectural elements are still recognisable in different outcrops exposed along the Santa Cruz coastal area and some examples will be discussed in the next sections.

The distribution and geometry of sandstone intrusions also depends on whether dominant regional tectonic stress fields are developed. Based on natural examples, and laboratory experiments which modelled unconsolidated homogeneous material as the host unit, it has been

demonstrated that intrusions tend to fill pre-existing tectonic structures, and that they predominantly form low to high angle dikes in tectonically active areas (Galland et al., 2003; 2007; Ferre' et al., 2012; Palladino et al., 2016; 2018) (Fig. 2b). Flat-lying intrusive geometries are still possible in compressional settings, when the maximum principal stress (σ_1) is horizontal and the minimum principal stress (σ_3) is vertical (Galland et al., 2003).

The SCIC extends for 15 km between the city of Santa Cruz and Davenport and for several km inland (Fig. 1). It consists of three different architectural elements termed the parent units, the intrusive network, and extrudites that will be described in the following sections. We also include sandstone intrusions within the SCIC that are emplaced along faults and are not temporally correlated with the majority of sandstone intrusions recognised in the study area.

3.2. Parent units

Although the parent-intrusion relationships are typically not well exposed, the Santa Margarita Sandstone is generally interpreted to be a parent unit (Boehm and Moore, 2002; Thompson et al. 2007). Multiple parent sandstone units were invoked by Clark (1981) for the SCIC using mineralogical data from exposures at Panther Beach/Yellowbank Creek localities (Fig. 1). The Pliocene Purisma Formation was identified in the Panther Beach/Yellowbank Creek localities as a parent unit based on similar overall composition and the occurrence of andesine feldspar, which has a volcanic provenance and is unknown in the Santa Margarita Sandstone (Scott et al., 2009). For the Purisima Formation (Early Pliocene; Norris, 1986) to form a parent unit would require either its juxtaposition below the Miocene Santa Cruz Mudstone at the time of sand injection, or a downwards injection direction from the Pliocene onwards.

3.3. The intrusive sand network

The SCIC has a widespread and well-developed intrusive network, which mainly consists of dikes and occasional sills. Saucer-shaped intrusions are also locally present. Single intrusions

generally range from a few centimetres to a decimetre thick, while isolated dikes or sills can locally be several metres thick. Although the distance from one large intrusion to another can be significant (in the order of tens or hundreds of metres), the presence of minor intrusions provides good connectivity throughout the injection network. Connectivity between sandstone intrusions is demonstrated by the common occurrence of tar that has migrated along the fractures cropping out in study area.

3.3.1. Dikes

Dikes are very well exposed in the study area, with key localities at 4 Mile Beach and Bonny Doon (Fig. 1). Within the general Santa Cruz coastal area, dikes are sub-vertical, or at high angles to bedding, and occur as single intrusions or swarms that are water and tar saturated (Fig. 3a-e). Single dikes vary in aperture from a few centimetres to more than 1m. Bifurcation (Fig. 3a), side-stepping and marked changes in orientation are common (Fig. 3b, c). Dikes are typically planar with sharp discordant margins with host strata, although undulating, irregular contacts also occur, usually in association with intensely fractured zones. Mudstone clasts of host strata commonly form “floating” textures in the sandstone dike matrix. These clasts are generally angular to slightly rounded and jigsaw textures occur (Duranti and Hurst, 2004) (Fig. 3d-e). The internal structure of the sandstone intrusions is characterised by mm- to cm-spaced banding. Dikes fall into three main trends that are oriented N-S, WSW-ENE and SW-NE (Fig. 3f).

3.3.2. Sills

Sills mainly crop-out at Panther Beach/Yellowbank Creek, while small-scale sills also occur at 4 Mile Beach (Fig. 1). Sills typically display low-angle (<5º) discordance with bedding (Fig. 4), and range in thickness from a few centimetres to several decimetres, with the exception of the Panther Beach/Yellowbank Creek locality where sills are up to ~20m in thickness (Thompson et al., 2007; Scott et al., 2009) (Fig. 1). Sill margins are irregular with lateral thickness variation and

abrupt lateral terminations. The lower contacts of sills are often erosive with scoured surfaces common, while upper boundaries are typically discordant with the host strata (Fig. 4a, b). These sharply discordant erosive contacts with overlying host strata conclusively demonstrate the intrusive origin of the sills. Meter to 10's of meters wide convex-up features, termed scallops (Hurst et al., 2005), are sometimes associated with dikes that emanate from them into the overburden. Mudstone breccias with jigsaw configuration of clasts, together with isolated mudstone rafts, occur along the upper and lower margins of sills. Internal sedimentary structures are dominated by mm- to dm-thick banding, which is oriented approximately parallel to the margins of the sandstone intrusions. Plane-parallel banding is also commonly observed (Fig. 4a, b). Within the thickest sills, sedimentary features including convolute lamination, fluid-escape structures and pipes suggest turbulent flow during emplacement (Scott et al., 2009).

3.3.3. Saucer-shaped intrusions

Saucer-shaped, tar-saturated sandstone intrusions are very well exposed at 4 Mile Beach (Fig. 1). In cross-section, they consist of inner bedding-parallel sandstone intrusions that are connected laterally with two outer sills by means of segments inclined at between 15° and 60° (Fig. 4c, d). Similar features observed on seismic images are often referred to as wings (Huuse et al., 2007, Jackson et al., 2011). Inner sills, that are typical of large saucer-shaped intrusions, are not observed (Huuse et al., 2007; Hurst and Vigorito, 2017). A nested geometry of saucers (Fig. 4c, d) occurs where smaller intrusions overlie large saucers and are linked by dikes with cuspate geometry (Fig. 4e, f). Saucer-shaped intrusions are 2 to 15 cm thick with undulating, stepped margins. Although sandstone intrusions probably comprise less than 10% of the rock volume, they provide excellent connectivity as demonstrated by the pervasive tar saturation.

3.3.4 Sandstone-filled faults

Sandstone intrusions emplaced directly along tectonic structures are a volumetrically small, and therefore frequently overlooked, characteristic of sandstone intrusion complexes (Palladino et al., 2016, 2018). In the SCIC, they are an integral part of the injection complex and predominantly consist of sandstone-filled normal faults (SFNF *sensu* Palladino et al., 2018) with sandstone intrusion along strike-slip and compressional fault planes being less common. We have recognized only a couple of examples of sand injection along strike-slip faults, and a few cases of compressional faults filled by sand. The number of normal faults is much greater as we will show in the following sections. Sandstone-filled normal faults (SFNF) are cm- to dm–wide, with small offsets, rarely developed shear zones and steeply-dipping attitudes.

Sandstone-filled normal faults are well exposed at Bonny Doon and Laguna Creek beaches (Fig. 1). At Bonny Doon Beach, a series of N-S and NNW-SSE oriented SFNF form a conjugate set that dissect the Santa Cruz Mudstone (Fig. 5a); a thin mudstone interval forms a useful marker bed (Fig. 5b). The master fault consists of a high angle SFNF with a maximum thickness of 30 cm and a throw of 15 cm. The entire exposure of the fault is propped open by a sandstone fill. A weak damage zone, consisting of closely-spaced fractures, is parallel to the fault margin. Unlike associated faults that are not intruded by sandstone and contain a fault gouge comprising cataclastic breccia and clay smear, the SFNF commonly lacks fault gouge. More details on deformation styles associated with faulted sand injection are in Palladino et al. (2018).

At Laguna Creek Beach, the outcrop has numerous normal fault planes that are characterised by intense cataclasis and clay smearing with occasional SFNF present. An almost vertical fault zone displays ~50 cm offset of a clay marker bed (Fig. 5c, d). The fault consists of two main fully-injected overlapping segments, which are connected by secondary *en echelon* linked fractures (Fig. 5e, f). Locally, these linked fractures have a sandstone fill. Most deformation is confined between the two fault segments whereas the external areas have very little evidence of brittle deformation. The role played by these structures in the evolution of the Santa Cruz petroleum system, and the relationships between sandstone-filled faults and the other elements of the SCIC are discussed in detail later.

3.4 *Sand extrudites*

Remarkable exposure of sand extrudites at Red, White and Blue Beach (Fig. 1) records phases of sand extrusion onto the paleo-seafloor (Hurst et al., 2006) (Fig. 6). They occur as tar-saturated, laterally-discontinuous, mounded sandstone units within the Santa Cruz Mudstone. Extrudites extend over hundreds of meters, are meters thick, and consist of sand bodies that display a well-developed bed-parallel lamination or cross-bedding (Fig. 6a, b). Locally, the original structure of sand volcanoes, which show multiple conduits and laminated flanks reaching inclinations approaching 30°, are still preserved. Planar basal surfaces are common, disturbed only by occasional sub-vertical 'escape' burrows.

4. Tectonic structures in the Santa Cruz area

In order to investigate the relationships that exist between tectonic structures and sandstone intrusions, a detailed structural survey has been carried out in five key outcrop locations: Shark Fin Cove, Bonny Doon Beach, Panther Beach, Laguna Beach and 4 Mile Beach (Fig. 1c). Tectonic structures mainly consist of large-scale open folds, meso-scale faults, and dilatant fractures and joints. According to our observations, and those of previous studies (Phillips, 1990), the structures are interpreted as a brittle expression of the Cenozoic tectonic deformation related to the San Gregorio and San Andreas faults (Fig. 1a, b).

4.1. Folds

Open anticlinal and synclinal folds with decametre to kilometre wavelength are recognised throughout the study area (Fig. 7a, b). They are characterised by gently-dipping limbs and fractured fold hinges. In outcrop, the fold hinge zone is often removed by erosion. Fold axes commonly display NW-SE trends and SE plunges, which is in general agreement with observations made by Phillips (1990) however, minor folds trending NE-SW and N-S, also occur (Fig. 7c).

4.2. Faults

Sets of differently oriented faults are the most prominent tectonic feature recognised along the coastal sector (Fig. 8a). Normal faults are the most common fault type, while strike-slip and occasional reverse faults are less common.

In general, normal faults consist of conjugate sets with a master fault plane and a series of minor associated antithetic and synthetic faults and fractures. Usually, major structures have small offsets, ranging from a few centimetres to some metres, and form a graben-like geometry (Fig. 8b). The best exposures of normal faults are found at 4 Mile Beach, Laguna Creek Beach and Bonny Doon Beach (Fig. 8c). Normal fault kinematics are characterised by dip-slip oriented slickensides coupled with stratigraphic offsets. Fault zones are commonly marked by fault breccia, together with fine-grained cataclastic crushed material. Clay smear is locally observed along the fault planes where they cut clay-rich horizons (Fig. 8d).

In common with the normal faults, strike-slip (Fig. 8e, f) and reverse faults (Fig. 8g, h) are characterised by limited displacement and narrow fault zones and are best exposed around 4 Mile and Bonny Doon beaches. Fault breccia is rarely present, although thin (cm-scale) cataclastic zones and striated fault planes occur locally.

Measurement of fault orientation at all locations allows us to identify several fault sets that display a range of orientations and kinematics (see stereoplots in Fig. 8). In general, conjugate sets of NNE-SSW, N-S, NNE-SSW and NE-SW trending faults consist of extensional faults (Fig. 8a-d), NW-SE and NNW-SSE trending faults comprise dextral strike slip faults (Fig. 8e-f), and E-W and WNW-ESE trending structures have either a contractional or less clear kinematic origin (Fig. 8g-h).

4.3. Fractures

Fractures form a pervasive network throughout the study area. In general, fracture density increases from centimetres to a few millimetres when approaching fault planes. Conversely, fractures are regularly distributed and more widely spaced (centimetres to a few tens of centimetres) in the intra-fault areas (Rizzo et al., 2017). Outcrops at 4 Mile and Panther beaches (Fig. 1) represent typical case study fracture scenarios for the studied area.

The cliff-line of 4 Mile Beach is an excellent location for the study of fracture geometry, and the interactions between fractures and sandstone intrusions. In particular, most of the outcrop consists of steep, vegetation-free walls and a series of raised, intertidal terraces that together provide an exceptional 'pseudo-three dimensional' outcrop. Fractures are generally connected by abutments (Y- or T- points *sensu* Manzocchi et al., 1998 and Manzocchi, 2002) or have cross-cutting relationships (Fig. 9a). Fracture length varies from a few centimetres to some decimetres, with an average length in the order of 20 cm (Rizzo et al., 2017). Fracture apertures average on the order of 3 (±2) mm. Linkages between different fractures occur by dilatational jogs, horsetail and, without any physical intersection, by means of *en echelon* arrays (Kim et al., 2004; Peacock et al., 2016). In cross-section, the fractures usually show X and S shaped geometries (Fig. 9b). Fracture meshes (Sibson, 1996) are also common (Fig. 9c). Observations of plumose structures with well-developed hackle fringes support the hypothesis that Mode I tensile fracturing is the main mechanism by which fractures opened. Local evidence for shear fracture mechanisms is provided by calcite-filled tension gashes. As fractures cross different lithologies, diffraction phenomena may occur. Commonly, tensional fractures are filled by a hydrocarbon residue of tar (Rizzo et al., 2017) (Fig. 9d), together with less common calcite infill (Fig. 9e). Fracture distribution at 4 Mile Beach has two major conjugate fracture sets trending NNW-SSE and NW-SE (Fig. 9f).

At Panther Beach (Fig. 1), closely-spaced fractures are well-exposed along a series of cliff sections that are similar to those at 4 Mile Beach. Here, the thick sandstone sill (Thompson et al., 2007; Scott et al., 2009) (Fig. 4a) shows a different style of fractures, with X-shaped geometry and mm-thick deformation bands, that isolate rhomboidal segments of sandstone (Fig. 9g). Millimetre-scale offsets typify fracture intersections. Fractures either terminate along, or are deflected by, finer grained, clay-rich layers. The fracture distribution displays predominantly NNW-SSE-orientations,

with NW-SE-oriented fractures also abundant, while NE–SW and E-W-striking trends are less evident (Fig. 9h).

4.4. Origin of tectonic structures in the Santa Cruz area

Studies of Pliocene-Quaternary tectonic structures in the San Francisco Bay area, which includes the Santa Cruz area, were performed by a number of authors (Wilcox et al., 1973; Aydin and Page, 1984; Page et al., 1998). Based on these studies, the orientations of the tectonic structures recognised in the study area are consistent with a "wrench tectonic" environment (Moody and Hill, 1956) developed under the control of the San Andreas (average azimuth N324°) and the San Gregorio (average azimuth N341°) dextral strike-slip fault zones (Aydin and Page, 1984; Phillips, 1990) (Fig. 1b). However, comparison between outcrop fault orientations with those produced in laboratory experiments also identified some inconsistencies as discussed in Aydin and Page (1984). Primarily, these inconsistencies are attributable to the orientation of tectonic structures not being the result of movement along a single major fault, but rather the result of different interacting major faults. Secondly, fault orientation also depends on the mechanical behaviour of the varying lithologies undergoing deformation. Finally, fracture orientation is affected by crustal heterogeneity and rotation during progressive shear.

Orientations of tectonic structures measured in the Santa Cruz coastal area show a close similarity with a structural model consisting of dextral strike slip faults oriented similar to the San Gregorio and San Andreas faults. The main ranges of fault trends recognised in the Santa Cruz Coastal area are illustrated in Fig. 10. NW-SE and NNW-SSE trending faults are interpreted as conjugate sets of strike-slip faults developed parallel to the San Andreas and the San Gregorio fault zones, whereas NNE-SSW oriented strike slip faults correspond to the associated Riedel structures (Fig. 8e, f). NNW-SSE, N-S, NNE-SSW and NE-SW trending extensional faults are dilational step-overs between right-lateral faults (Fig. 8b, c).

Unlike extensional and strike slip faults, SW-NE and WSW-ENE trending contractional faults (Fig. 8g, h) are inconsistent with a wrench tectonic model. However, they could be an

expression of compressional deformation connected with the development of the Santa Cruz homocline between the Ben Lomond Mountains and the San Gregorio Fault (Stanley, 1990). According to Phillips (1990), southwest-plunging folds may be related to differential compaction mechanisms between thick sedimentary beds of the Santa Margarita Sandstone and the overlying Santa Cruz Mudstone.

Fracture orientations largely reflect the trends of the main faults. For example, at 4 Mile and Panther beaches (Fig. 9), most of the N-S, NNE-SSW and NE-SW oriented fractures are consistent with the dominant extensional fault trends throughout the area. Similarly, NNW-SSE and NW-SE fracture orientations are consistent with the dextral strike-slip faults. The NE–SW trends could however be associated with outer-arc axial fracturing related to the folding phase. As fractures that accompany the emplacement of the sandstone intrusions are distributed along well-defined trends, we exclude a possible hydraulic fracturing origin that would typically show less constrained orientations (Hurst et al., 2011).

5. Relationships between sandstone intrusions and tectonic structures

In the previous sections we described the main characteristics and spatial distribution of sandstone intrusions and tectonic structures occurring in the Santa Cruz coastal area. Field observations allowed us to recognise sandstone intrusions that are either related, or unrelated, to tectonic structures that are now discussed.

5.1. Sandstone intrusions associated with tectonic structures

Close relationships between sandstone intrusions and tectonic structures have already been ascertained by the recognition in the study area of sandstone-filled normal faults (Phillips, 1990; Palladino et al., 2018) (Fig. 5). This evidence clearly indicates that fluidised sand was driven along tectonic discontinuities. The influence of tectonics on the distribution of sandstone intrusions is evident when comparing dike orientations with fault and fracture patterns (Fig. 10a, b). Although

sandstone dikes are spatially more dispersed than the orientation of the major faults, their orientation follows broadly similar trends of NNW-SSE, N-S, SW-NE and WSW-ENE, which are consistent with the average fault and fracture orientations. Notably, all dominant trends coincide with dilational structures. In particular, the majority of NNW-SSE, N-S and SW-NE oriented structures are compatible with extensional faults, whereas WSW-ENE oriented structures likely coincide with outer-arc extension fractures related to folding (Fig. 7). A small number of injections coincide with strike slip or contractional faults in which dilation is commonly inhibited.

5.2. Sandstone intrusions not associated with tectonic structures

The occurrence of sandstone-filled faults and fractures noted above markedly contrasts with sandstone intrusions which are unrelated to tectonics (Thompson et al., 1999; Boehm and Moore, 2002, Scott et al., 2009). These intrusions are interpreted to be emplaced in propagating hydraulic fracture network systems that formed during periods of severe, sometimes supra-lithostatic, pore-fluid pressure in the very shallow crust (Hurst et al., 2011). These sand injections are clearly overprinted by tectonics and do not show intrusion-parallel fractures that progressively increase toward dike margins, as expected for tectonically-related intrusive geological bodies (Delaney et al., 1986). Evidence for tectonic overprint of sandstone intrusions are particularly well-exposed at 4 Mile Beach, Shark Fin Cove and Laguna Beach.

At 4 Mile Beach, saucer-shaped sandstone intrusions are intensely overprinted by closely-spaced fractures which are genetically associated with larger extensional faults (Fig. 11a, b). We found no evidence of hydrofracturing and polygonal faults (Cartwright et al., 2003; Vigorito et al., 2008; Vigorito and Hurst, 2010) that are generally invoked as the mechanism which accommodates the emplacement of sandstone intrusions in sedimentary basins unaffected by tectonic deformation. Fractures systematically cut through the sandstone intrusions and continue into the host strata, indicating that the deposits were well-consolidated at the time when tectonic deformation occurred.

Of particular interest, is the 1.5 m thick sandstone dike cropping out in three adjacent locations at Shark Fin Cove (Fig. 11c). At two of the locations, the dike has planar margins, sharp contacts with the host strata, and no evidence of dike-parallel fracturing or mechanical brecciation, as typically associated with a fault plane (Fig. 11d). By contrast, at the third outcrop, the dike is significantly affected by post-emplacement deformation (Fig. 11e-f). In this case, deformation is concentrated along the dike margins, resulting in their reactivation. Occurrence of slickensides along the dike surfaces adds support to this interpretation. Here, stress concentration is accommodated differently by the mudstone and sandstone: in the brittle mudstone, deformation caused pervasive, intense fracturing that produced chaotic fine-grained cataclastic material; in the poorly-lithified sandstone, deformation produces conjugate, widely-spaced fracture sets (Fig. 11d).

A 1.5 m wide dike at Laguna Beach (Fig. 1) has evidence of post-emplacement vertical compression associated with regional extensional faulting (Fig. 11g). Consequently, we can interpret the observed conjugate fractures and shear surfaces that dip at 45° from the vertical (Fig. 11h) as structures formed by a vertical maximum principle stress (σ_1) that acted upon the poorly-consolidated sandstone. Prevailing arrays of NW-dipping shear planes caused the partial sinistral offset of the dike (Fig. 11h). In the mudstone host strata, brittle deformation mostly formed fractures, whereas in the sandstone deformation was accommodated mainly through conjugate deformation bands, with millimetre to centimetre offsets. When crossing the boundary separating the host strata from the dike, tectonic discontinuities are often refracted.

5.3. Cross-cutting relationships

Assuming a relatively synchronous faulting event in the Santa Cruz area, then the critical observations are: a) faults and associated fractures overprint and deform pre-existing sandstone intrusions, and, b) sand is injected along fault and fracture planes. These relationships make it unlikely that the SCIC was built during a single-stage emplacement event. Rather, the data shown in this work demonstrate that the present architecture of the SCIC results from distinct emplacement events. It follows that, two contrasting styles of sand injection are recorded in the

Santa Cruz area, the earliest associated with hydraulic fracturing in the very shallow crust (<250 m burial, Vigorito and Hurst, 2010), that was followed by a later injection event guided by tectonics, cross-cutting the earlier intrusion suites. The same brittle deformation phase caused the definitive failure of the hydrocarbon top seal.

The early sandstone intrusions form an assorted suite consisting of both high and low-angle dikes, sills and saucer-shaped sandstone intrusions (Fig. 4). This event is recorded by a series of extrudites documented by Hurst et al. (2006). The second generation of sandstone intrusions is emplaced along pre-to-syn-tectonic structures.

Clear cross-cutting relationships between the two recognised generations of sandstone intrusions are well-exposed at Panther Beach (Fig. 12). Here, in the south-eastern side of the beach, the first generation of sandstone intrusions is cut by sandstone-filled faults (Fig. 12a). The outcrop consists of a cliff made of diatomaceous mudstone hosting a 10cm thick, tar-saturated, low-angle dike belonging to the first generation of sandstone injections (Fig 12b). The dike has a reasonably constant lateral thickness, internal sedimentary structures, as well as bed-parallel mm-thick banding and no evidence of hydrofracturing associated with its emplacement. The dike is repeatedly cut by a series of conjugate sandstone-filled normal faults (Fig. 12c) showing offsets of a few centimetres.

One of the through-going faults named Fault 1 (Fig. 12b), visible on the right-hand side of the outcrop, offsets the low-angle dike by about 10 cm. A closer examination of the fault plane (Fig. 12d) highlights a very complex geometry; it mainly consists of several fault planes connected by linking damage zones represented by extensional fractures and dilatational jogs. Locally, these structures are filled by the sand which is likely to have been produced by the partial fluidisation of the faulted sand bodies. Where the fault intercepts the marker bed, the latter appears stretched and thinned rather than sharply cut by the tectonic structure.

We can identify three different zones along the faulted dike. In the inner zone (Fig. 12 e, f), in the proximity of the fault plane, the sand is structureless and contains floating clasts derived from the host strata. This characteristic indicates that fluidization processes predominantly

occurred during faulting in this portion. In the intermediate zone (Fig. 12 e, f), the dike is largely affected by fracturing (in a conjugate geometry) which overprints the original banding. Such features suggest that in this zone, the sand composing the dike was able to retain the tectonic structures and was not fluidised at the time of the deformation. In the external zone (Fig. 12 e, f), the lack of deformation structures and the occurrence of well-preserved bed-parallel banding indicates that this zone was unaffected by deformation. This lateral distribution clearly suggests that the faulted sandstone dike behaves in a progressively more ductile manner approaching the fault plane. In contrast, the host rock shows a brittle behaviour as testified by the occurrence of pervasive fractures.

A second fault zone, named Fault 2 (Fig. 12g), clearly offsets the low-angle dike with a different deformation style compared to Fault 1. In this case there is no evidence of ductile deformation and sand remobilisation along the exposed section. However, syn-/post-faulting sandstone intrusions occurred along a series of *en echelon* dilation fractures associated with the main fault plane (Fig. 12h, i). In this case, the fluidised sand might have been generated in distant portions of the fault and be laterally transported along dilational jogs.

The last fault zone, named Fault 3 (Fig. 12k), consists of a steeply-dipping normal fault discontinuously filled by tar-saturated sandstone. The fault plane shows a stepped geometry and sandstone intrusions mainly occur in correspondence with releasing steps which form lozenge-shaped cavities (Fig. 12l). Sandstone intrusions are also present along vertical fractures and minor fault planes associated with the main structure. The sandstone-filled structure cuts the low-angle dike and the offset is about 10 cm.

6. Discussion

6.1. Evolutionary model of the Santa Cruz Injection Complex

Previous attempts to comprehend both the potential of the Santa Cruz petroleum system (SCPS) and the distribution of the local paleo-stress have led to studies focussing on the

organization of the SCIC, and the relationships between the sandstone intrusions and tectonic structures (Clark, 1981; Phillips, 1981; 1990; Thompson et al., 1999; Boehm and Moore, 2002). In most of these studies, the regional tectonic stresses were inferred to control the emplacement of sand injections, which, in turn, influenced hydrocarbon accumulation. Field observations clearly reveal that, in places, dikes are intruded along faults. Phillips (1981; 1990) originally noticed the correspondence between fault and dike orientations, and therefore suggested that the emplacement of sandstone intrusions was mainly related to tectonic processes. Later, Thompson et al. (1999) confirmed the occurrence of sand injections along faults and fractures, however these authors also observed episodes of faulting that post-date sandstone intrusion at Yellowbank Creek. Boehm and Moore (2002) recognised a predominant NE-SW trend for the Santa Cruz sandstone intrusions, thus supporting the hypothesis of a strong tectonic control for sand injections. Similar to Thompson et al. (1999), they also provided evidence of faulting and fracturing that post-dates the sand injections. However, Boehm and Moore (2002) described a mechanical inconsistency represented by the emplacement of north-east-striking dikes, which would require a NW-SE minimum principal stress orientation (σ_3), and the simultaneous intrusion of sills, which suggests a sub-vertical minimum principal stress. The authors solved this apparent inconsistency by proposing a model where dikes intruded perpendicularly to the NW-SE oriented σ_3, and simultaneously weak sediment cohesion of the host rock allowed sills to be emplaced parallel to bedding (i.e. pre-existing bedding-parallel weakness). Notably, these previous works considered the emplacement of the SCIC to be the result of a single injection event.

Based on the data presented in the previous sections, and in particular on the detailed cross-cutting relationships, it is possible to explain the inconsistencies raised by Boehm and Moore (2002) in terms of a model involving two separate phases of sand injection from the Upper Miocene onwards (Fig. 13). Although these two events involved the same stratigraphic unit, i.e. the Santa Cruz Mudstone, the mechanical response of the sedimentary sequence and the regional tectonic controls varied between the two injection events, thereby resulting in sandstone intrusions displaying different characteristics.

The first injection event (Fig. 13a) caused the partial fluidisation of the Santa Margarita Sandstone and the emplacement of a significant volume of remobilised sand into the overlying top seal unit represented by the Santa Cruz Mudstone. This injection event mainly led to the emplacement of sills, saucer-shaped intrusions and some low-angle dikes as seen at 4 Mile Beach and Panther Beach (Fig. 4). Isolated dikes locally connected flat-lying sandstone intrusions positioned at different stratigraphic levels in the Miocene succession.

The energy released during this event was large enough to create fluid-pressure gradients between buried sand bodies and the basin floor. This resulted in the development of a complete sand injection complex, spanning remobilised parent units, intrusive elements and extrudites (Hurst et al., 2006; Vigorito and Hurst, 2010). Sills and saucer-shaped intrusions were emplaced at the depth where the vertical pore-fluid pressure gradient is equal to, or exceeds the overburden pressure, resulting in the minimum principal stress (σ_3) being vertical.

Evidence for this first top seal failure event, and initiation of the sand injection complex, are provided by the occurrence during the Miocene of sheet or mounded sandstones at Red and White Blue Beach (Fig. 1), which are interpreted as extrudites (Boehm and Moore, 2002; Hurst et al., 2006). In the field, no evidence for hydraulic fracturing attributable to this first event has been recognised. The lack of fractures is possibly related to the host strata still being poorly consolidated at the time of sand injection. If any fracture network did develop at this time, it behaved as a valve for the temporary passage of water and fluidised sands, thereby allowing overpressure to be dissipated. However, due to the unconsolidated state of the host unit, fractures were likely resealed soon after the sand emplacement. Later, diagenetic processes, leading to the litification of the host mudrock and entrapment of the injected sandstones, allowed the accumulation of hydrocarbons in the SCPS (Fig. 13b). In addition, once Opal A/Opal CT transformation involved the Santa Cruz Mudstone (El-Sabbagh and Garrison, 1990), most of the remaining fractures disappeared obliterating any evidence of hydraulic fracturing processes.

Several factors, in addition to rapid burial and regional tectonics, may have contributed to the build-up of the necessary fluid pressure. According to laboratory experiments (Galland et al., 2003) (Fig. 2), the occurrence of flat-lying sandstone intrusions, as well as sill and saucer-shaped

intrusions indicates the absence of oriented tectonic stresses, or, more probably, the development of a horizontal maximum principal stress which led to the folding of the Miocene succession. According to Phillips (1990), differential compaction and compressional tectonics created folding suitable for hydrocarbon migration and accumulation. This event could have also triggered sandstone injections as many intrusions are concentrated along the crest of the anticlines (Thompson et al. 1999; Boehm and Moore, 2002). In this context, sand injections cropping out at Major Creek (Fig. 1), one of the most extensive injected sand bodies and previously exploited for tar mining, corresponds with the crest of a major SW-plunging anticline.

Following this event, the system resealed, and the depositional and injected sandstones collectively created a permeable network allowing further hydrocarbon accumulation.

The second injection event (Fig. 13c) caused sand fluidisation and remobilization of both the Santa Margarita Sandstone and the previously injected sandstone intrusions. At this time, it is likely that the Purisima Formation sandstones were also affected by remobilization processes providing sandstone intrusions in the Panther Beach/Yellowbank Creek area. The new sand injections mainly consist of a series of high angle dikes, emplaced along extensional faults and fractures, consistently following the trend of the San Andreas/San Gregorio fault system (Fig. 8), cutting through the Santa Cruz Mudstone that were by this time fully lithified. The sudden failure and re-opening of the system caused a rapid fluid transfer from the underlying overpressured units into the newly-formed structures, according to the mechanism proposed by Palladino et al. (2018). Sandstone-filled faults and brittle deformation accompanying this injection phase clearly post-date sandstone intrusions created during the first event (Fig. 12). We then suggest that this fault system reached the basin floor or the topographic surface, breaking the top seal and triggering the consequent leak of the hydrocarbons. This chain of events is documented by the widespread occurrence of tar-saturated sandstones and fractures currently observed at Santa Cruz. Extrudites may also have been produced during this event but, unfortunately, recent erosional surfaces (Weber and Allwardt, 2001) cut the studied outcrops, and do not allow a precise age constraint for this faulting/injection event.

6.2. Implication for seal bypass system

The second event described in the proposed model records the failure of the SCPS top seal due to the occurrence of seal bypass systems. Seal bypass systems described by Cartwright et al. (2007) are classified into three main groups of geological structures: i) fault related, ii) intrusion related, and iii) pipe related. All these elements cause the breach of the sealing sequences and allow fluids to leak across the seal. As frequently happens, categorizing geological structures often represents an oversimplification of the phenomena observed in nature, and the Santa Cruz coastal area is no exception regarding seal bypass systems. In fact, our case study of the SCPS reveals that seal bypass systems can be created by hybrid geological structures formed between two end members. In this specific case, we consider the sandstone-filled normal faults to be the result of combining fault related and intrusion related seal bypass systems. We believe that this is applicable not only for sandstone-filled normal faults, but for all sandstone-filled faults and, as increasing numbers of these structures are recognized, they must be considered when exploring intrusive reservoirs.

7. Conclusions

We have performed a detailed study of sandstone intrusions that are well-exposed along the coast between Santa Cruz and Davenport in Central California, and this has enabled us to unravel the evolutionary history of the Santa Cruz petroleum system (Phillips, 1990; Hosford Scheirer et al., 2013). This study builds on earlier work on sandstone-filled normal faults (e.g. Palladino et al., 2018) and focuses on the paradox that sandstone intrusions generated in the study area may be either related, or indeed unrelated, to regional tectonic structures.

To better understand the relationships developed between tectonic structures and sandstone intrusions, the case study involved a detailed structural analysis of fractures, faults and fold axes, combined with an investigation of the orientation of the outcropping sandstone intrusions. This analysis allows us to recognise that the Santa Cruz Injection Complex (SCIC) is

the result of two distinct emplacement events that initiated in the Late Miocene, and is summarized in the following two-stage evolutionary model for the Santa Cruz petroleum system (Fig. 13).

During the first phase, the failure of the top seal, represented by the Santa Cruz Mudstone, led to the emplacement of a series of sills, saucer-shaped intrusions and dikes under the control of compaction and compressional tectonic processes. The emplacement of additional sand enhanced the permeability of the Santa Cruz Mudstone and allowed hydrocarbon accumulation. The lack of brittle deformation features associated with this first event testifies that sand injection occurred in a poorly consolidated host rock (i.e. the Santa Cruz Mudstone) and that the fractures resealed after sand emplacement. The healing of the fracture system enabled the accumulation and entrapment of hydrocarbons and building of the Santa Cruz petroleum system. Stratigraphic relationships around sandstone extrudites allow us to attribute this event to the Late Miocene.

The second phase of sand injection was closely associated with brittle tectonic events and is supported by the presence of sand bodies emplaced along high-angle extensional faults. Brittle deformation accompanying this event indicates that sand injection occurred in well-consolidated host strata. This event, whose age is still uncertain but ranges between the Late Miocene to Quaternary, caused a breaching of the top seal and the leaking of hydrocarbons previously accumulated in the Santa Cruz petroleum system. Most of the deformation is accommodated via normal faulting and widespread fracturing. Analysis of the trends of these structures shows that they are consistent with wrench tectonics and are compatible with the regional deformation that was predominantly controlled by the San Gregorio and the San Andreas fault zones.

Acknowledgements

We acknowledge the reviews of three anonymous referees and are also very grateful to Andrew Hurst and David Iacopini for their critical comments of an earlier version of the paper. We also wish to thank Denis Bureau and Antonella Gatto for their support in the field.

References

Atwater, T., Stock, J., 1998. Pacific-north America plate tectonics of the Neogene southwestern United States: an update. Int. Geol. Rev. 40, 375-402.

Aydin, A., Page, B.M., 1984. Diverse Pliocene-Quaternary tectonics in a transform environment, San Francisco Bay region, California. GSA Bulletin 95, 1303-1317.

Barron, J.A., 1986. Paleoceanographic and tectonic controls on deposition of the Monterey Formation and related siliceous rocks in California. Palaeogeography, Palaeoclimatology, Palaeoecology 53, 27-45.

Boehm, A., Moore, J.C., 2002. Fluidized sandstone intrusions as an indicator of paleostress orientation, Santa Cruz, California. Geofluids 2, 147-161.

Brabb, E.E., 1989. Geologic map of Santa Cruz County, California: U.S. Geological Survey Miscellaneous Investigations Series Map I-1905, scale 1:62,500 (1 sheet).

Bradley, W.C., Griggs, G.B., 1976. Form, genesis, and deformation of central California wave-cut platforms. Geological Society of America Bulletin 87, 433-449.

677 Bürgmann, R., Arrowsmith, R., Dumitru, T., McLaughlin R., 1994. Rise and fall of the southern
678 Santa Cruz Mountains, California, from fission tracks, geomorphology, and geodesy. J. Geophys.
679 Res. 99, 20181–20202, doi:10.1029/94JB00131.

680

681 Cartwright, J., James, D. & Bolton, A., 2003. The genesis of polygonal fault systems: a review, in:
682 Van Rensberger, P., Hillis, R.R., Morley, C.K. (Eds.), Subsurface Sediment Mobilization.
683 Geological Society, London, Special Publications 216, 223–243.

684

685 Cartwright, J.A., Huuse, M., Aplin, A., 2007. Seal bypass systems. AAPG Bulletin 91, 1141–1166.

686

687 Clark, J.C., Rietman, J.D., 1973. Oligocene stratigraphy, tectonics, and paleogeography southwest
688 of the San Andreas fault, Santa Cruz Mountains and Gabilan Range, California Coast Ranges:
689 U.S. Geological Survey Professional Paper 783, 18 p.

690

691 Clark, J.C., 1981. Stratigraphy, palaeontology, and geology of the central Santa Cruz Mountains,
692 California Coast Range: U.S. Geological Survey Professional paper 1168, p. 51.

693

694 Delaney, P.T., Pollard, D.D., Ziony J.I., McKee E.H., 1986. Field relations between dikes and joints
695 emplacement processes and paleostress analysis. Journal of Geophysical Research 91, 4920-
696 4938.

697

698 Dickinson, W.R., Ducea, M., Rosenberg, L.I., Greene, H.G., Graham, S.A., Clark, J.C., Weber,
699 G.E., Kidder, S., Ernst, W.G., Brabb, E.E., 2005. Net dextral slip, Neogene San Gregorio–Hosgri

fault zone, coastal California: Geologic evidence and tectonic implications: Geological Society of America Special Paper 391, 43 p. doi: 10.1130/2005.2391.

Dixon, R.J., Schofield, K., Anderton, R., Reynolds, A.D., Alexander, R.W.S., Williams, M.C., Davies, K.G., 1995. Sandstone diapirism and clastic intrusion in the Tertiary submarine fans of the Bruce-Beryl Embayment, Quadrant 9, UKCS, in: Hartley, A.J., Prosser, D.J. (Eds.), Characterisation of deep-marine clastic systems: Geological Society, London Special Publication 94, 77–94.

Duranti, D., Hurst, A., Bell, C., Groves, S., Hanson, R. 2002. Injected and remobilised Eocene sandstones from the Alba Field, UKCS: core and wireline log characteristics. Petrol. Geosci. 8, 99–107.

Duranti, D., Hurst, A., 2004. Fluidization and injection in the deep-water sandstones of the Eocene Alba formation (UK North Sea). Sedimentology 51, 503-529.

Eldridge, G.H., 1901. The asphalt and bituminous rock deposits of the United States: U.S. Geological Survey Ann. Rept. 22, pt. 1, 209-464.

El-Sabbagh, D., Garrison, R.E., 1990. Silica digenesis in the Santa Cruz Mudstone (Upper Miocene), La Honda Basin, California, in: Garrison, R.E., Greene, H.G., Hicks, K.R., Weber G.E., Wright T.L. (Eds.), Geology and Tectonics of the Central California Coast Region, San Francisco to Monterey, Volume and Guidebook, Pacific Sec. Assoc. Amer. Petrol. Geol., 123–132.

Ferre', E.C., Galland, O., Montanari, D., Kalakay, T.J., 2012. Granite magma migration and emplacement along thrusts. Int. J. Earth Sci. Geol. Rundschau Springer. http://dx.doi.org/10.1007/s00531-012-0747-6.

Galland, O., De Bremond d'Ars, J., Cobbold, P.R., Hallot, E., 2003. Physical models of magmatic intrusion during thrusting. Terra Nova 15, 405-409.

Galland, O., Cobbold, P.R., De Bremond d'Ars, J., Hallot, E., 2007. Rise and emplacement of magma during horizontal shortening of the brittle crust: insights from experimental modelling. J. Geophys. Res. 112, B06402. http:// dx.doi.org/10.1029/2006JB004604.

Hallmark, R.O., 1980. Unconventional petroleum resources in California: Calif. Div. Oil and Gas Pub. TR25, 17 p.

Heck, R.G., Edwards, E.B., Kronen, J.D., Jr., Willingham, C., 1990. Petroleum potential of the offshore outer Santa Cruz and Bodega basins, California, in: Garrison, R.E., Greene, H.G., Hicks, K.R., Weber, G.E., Wright, T.L. (Eds.), Geology and tectonics of the Central California Coast Region—San Francisco to Monterey. American Association of Petroleum Geologists, Pacific Section, Calif., 143-163.

Hosford Scheirer, A., Magoon, L.B., Graham, S.A., 2013. Petroleum Systems of the Santa Cruz County Coast, California. AAPG Search and Discovery Article, Pacific Section AAPG, SPE and SEPM Joint Technical Conference, Monterey, California.

748 Hurst, A., Cartwright, J. A., Huuse, M., Jonk, R., Schwab, A., Duranti, D., Cronin, B., 2003.
749 Significance of large scale sand injectites as long-term fluid conduits: Evidence from seismic data.
750 Geofluids 3, 263–274.

751

752 Hurst, A., Cartwright, J.A., Duranti, D., Huuse, M., Nelson, M., 2005. Sand injectites: an emerging
753 global play in deep-water clastic environments, in: Doré, A., Vining, B. (Eds.), Petroleum Geology:
754 North-west Europe and Global Perspectives. Proceedings of the 6th Petroleum Geology
755 conference. Geological Society, London, 133–144.

756

757 Hurst, A., Cartwright, J.A., Huuse, M., Duranti, D., 2006. Extrusive sandstones (extrudites): a new
758 class of stratigraphic trap?, in: Allen, M.R., Goffey, G.R, Morgan, R.K., Walker, I.M. (Eds.), The
759 deliberate search for the stratigraphic trap. Geological Society, London, Special Publications 254,
760 289-300.

761

762 Hurst, A., Scott, A., Vigorito, M., 2011. Physical characteristics of sand injectites. Earth Sci. Rev.
763 106, 215-246.

764

765 Hurst, A., Vigorito M., 2017. Saucer-shaped sandstone intrusions: An underplayed reservoir target.
766 AAPG Bulletin 101, 625–633.

767

768 Huuse, M.J., Cartwright, J.A., Hurst, A., Steinsland, N., 2007. Seismic characterization of large-
769 scale sandstone intrusions, in: Hurst, A., Cartwright, J. (Eds.), Sand Injectites: Implications for
770 Hydrocarbon Exploration and Production: American Association of Petroleum Geologists Memoir,
771 Tulsa, 21–35.

Jackson, C.A.L., Huuse, M., Barber, G.P., 2011. Geometry of wing-like intrusions adjacent to a deep-water slope channel complex and implications for hydrocarbon exploration and production: a 3D seismic case from the Maloy Slope, offshore Norway. AAPG Bull. 95, 559-584.

Jenkins, O.P., 1930. Sandstone dikes as conduits for oil migration through shales. AAPG Bull. 14, 411-421.

Jolly, R.J.H., Lonergan, L., 2002. Mechanisms and controls on the formation of sand intrusions. J. Geol. Soc. Lond. 159, 605-617.

Kim, Y., Peacock, D.C.P., Sanderson, D.J., 2004. Fault damage zones. J. Struct. Geol. 26, 503-517.

Lillis, P.G., Stanley, R.G., 1999. Petroleum systems of the La Honda Basin, California. AAPG Bulletin 83, 694-694.

Lowe, D.R., 1975. Water escape structures in coarse-grained sediments. Sedimentology 22, 157–204.

Manzocchi, T., Ringrose, P.S., Underhill, J.R., 1998. Flow through fault systems in high-porosity sandstones, in: Coward, M.P., Daltaban, T.S., Johnson, H. (Eds.), Structural Geology in Reservoir Characterization. Geological Society, London, Special Publications 127, 65-82.

Manzocchi, T., 2002. The connectivity of two-dimensional networks of spatially correlated fractures, Water Resour. Res. 38, 1162. doi:10.1029/2000WR000180

Molyneux, S., 1999. Giant clastic dykes and sills of Santa Cruz, Coastal California. Petroleum Exploration Society of Great Britain, Newsletter, 118–125.

Molyneux, S., Cartwright, J. A., Lonergan, L., 2002. Conical amplitude anomalies as evidence for large scale sediment intrusions. First Break 20, 123–129.

Moody, J.D; Hill, M.J., 1956. Wrench-fault tectonics. GSA Bulletin 67, 1207-1246.

Mullins, H.T., Nagel, D.K., 1982. Evidence for shallow hydrocarbons offshore northern Santa Cruz County, California. Bull. Am. Assoc. Pet. Geol. 66, 1130-1140.

Newsom, J.F., 1903. Clastic dikes. Geological Society of America Bulletin 14, 227–268.

Page, B.M., Holmes, C.N., 1945. Geology of the bituminous sandstone deposits near Santa Cruz County, California: U.S. Geological Survey Oil and Gas Investigations Preliminary Map 27.

Page, B.M., Thompson, G.A., Coleman, R.G., 1998. Late Cenozoic tectonics of the central and southern coast ranges of California. Geol. Soc. Am. Bull. 110, 846-876.

Palladino, G., Grippa, A., Bureau, D., G. Ian, Alsop, Hurst, A., 2016. Emplacement of sandstone intrusions during contractional tectonics. Journal of Structural Geology 89, 230-249.

Palladino, G., G. Ian, Alsop, Grippa, A., Zvirtes G., Philipp R.P., Hurst, A., 2018. Sandstone-filled normal faults: A case study from central California. Journal of Structural Geology 110, 86–101.

Peacock, D.C.P., Nixon, C.W., Rotevatn, A., Sanderson, D.J., Zuluaga, L.F., 2016. Glossary of fault and other fracture networks. Journal of Structural Geology 92, 12-29.

Phillips, R.L., 1981. Depositional and structural controls on heavy-petroleum tar sands in Santa Cruz Mountains. AAPG Bull. 65. p. 970.

Phillips, R.L., 1990. Depositional and structural controls on the distribution of tar sands in the Santa Cruz mountains, California, in: Garrison, R, Greene, H.G., Hicks, K.R., Weber, G.E., Wright, T.L. (Eds.), Geology and Tectonics of the Central California Coastal Region, San Francisco to Monterey, Volume and Guidebook, Pacific Section, American Association of Petroleum Geologists, Pacific Section, Bakersfield, CA, Book GB67, 105–21.

Phizackerley, P.H., Scott, L.O., 1978. Major tar-sand deposits of the world, in: Chilingarian, G.V., (Ed.), Bitumens, Asphalts, and Tar Sands, 57-92.

Rizzo, R.E., Healy, D., De Siena, L., 2017. Benefits of maximum likelihood estimators for fracture attribute analysis: Implications for permeability and up-scaling. Journal of Structural Geology 95, 17-31.

Ross, J.A., Peakall, J., Keevil, G.M., 2014. Facies and flow regimes of sandstone-hosted columnar intrusions: Insights from the pipes of Kodachrome Basin State Park. Sedimentology 61, 1764–1792.

Scott, A., Vigorito, M., Hurst, A., 2009. The process of sand injection: internal structures and relationships with host strata (Yellowbank Creek Injectite Complex, California, U.S.A.). Journal of Sedimentary Research 79, 568–583.

Scott, A., Hurst, A., Vigorito, M., 2013. Outcrop-based reservoir characterization of a kilometer-scale sand-injectite complex. AAPG Bull. 97, 309-343.

Sherry, T.J., Rowe, C.D., Kirkpatrick, J.D., Brodsky, E.E., 2012. Emplacement and dewatering of the world's largest exposed sand injectite complex. Geochemistry, Geophysics, Geosystems 13, 1-17.

Sibson, R.H., 1990. Conditions for fault-valve behaviour. In: Knipe, R.J., Rutter, E.H. (Eds.), Deformation Mechanisms, Rheology and Tectonics, Geological Society, London Special Publications, 54, 15–28.

Sibson, R.H., 1996. Structural permeability of fluid-driven fault-fracture meshes. Journal of Structural Geology 18, 1031-1042.

Stanley, R.G., McCaffrey, R., 1983. Extent and offset history of the Ben Lomond Fault, Santa Cruz County, California, In: Andersen, D.W., Rymer, M.J. (Eds.), Tectonics and Sedimentation Along Faults of the San Andreas System. SEPM—Society of Economic Paleontologists and Mineralogists, Los Angeles, California, 79– 90.

Stanley, R.G., 1990. Evolution of the Tertiary La Honda Basin, central California, in: Garisson, R.E. et al. (Eds.), Geology and Tectonics of the Central California Coastal Region, San Francisco to Monterey, Guidebook, Am. Assoc. of Pet. Geol., Bakersfield, Calif., 67, 1–29.

Thompson, B.J., Garrison, R.E., Moore, J.C., 1999. A late Cenozoic sandstone intrusion west of Santa Cruz, California: Fluidized flow of water- and hydrocarbon saturated sediments, in: Garrison, R.E. Aiello I.W., Moore, J.C. (Eds.), Late Cenozoic fluid seeps and tectonics along the San Gregorio fault zone in the Monterey Bay region, California: Pacific Section AAPG Volume and Guidebook GB-16, p. 53–74.

Thompson, B.J., Garrison, R.E., Moore, C.J., 2007. A reservoir-scale Miocene Injectite near Santa Cruz, California, in: Hurst, A., Cartwright, J. (Eds.), Sand Injectites: Implications for Hydrocarbon Exploration and Production: American Association of Petroleum Geologists, Memoir 87, 151–162.

Vigorito, M., Hurst, A., Cartwright, J., Scott, A., 2008. Regional-scale shallow crustal remobilization: processes and architecture. Geol. Soc. Lond. Spec. Publ. 165, 609-612.

Vigorito, M., Hurst, A., 2010. Regional sand injectite architecture as a record of pore pressure evolution and sand redistribution in the shallow crust: insights from the Panoche Giant Injection Complex, California. J. Geol. Soc. Lond. 167, 889-904.

Weber, G.E., Allwardt, A.O., 2001. The geology from Santa Cruz to Point Año Nuevo: The San Gregorio fault zone and Pleistocene marine terraces: U.S. Geological Survey Bulletin, 2188, p. 1–32.

Wilcox, R.E., Harding, T.P., Seely, D.R. 1973. Basic Wrench Tectonics. AAPG Bulletin 57, 74-96.

Figure captions

Fig. 1 a) Sketch map of California including the location of the study area (red box) and the main tectonic structures represented by the San Andreas Fault Zone (SAFZ) and the San Gregorio Fault Zone (SGFZ). b) Schematic structural map. The study area is included between the Ben Lomond and the San Gregorio fault zones. c) Geological map of the study area (modified from Boehm and Moore, 2002). Outcrop locations and places referred to in the text are also shown. d) Stratigraphic column of the geological units cropping out in the Santa Cruz coastal area (modified from Boehm and Moore, 2002).

Fig. 2 a) Schematic organization of a sandstone intrusion complex following Vigorito and Hurst (2010). Dikes mainly occur in the lower and upper portion of the sequence. Sills are common in the middle portion. b) Possible geometries obtained for tectonically-unrelated and tectonically-controlled intrusions based on laboratory experiments (modified from Galland et al., 2007).

Fig. 3. Main characteristics of the dikes forming the SCIC. a) Bifurcating dike exposed at low tide in 4 Mile Beach. b) Photograph and interpretative line drawing (c) of dike swarm observable at Bonny Doon Beach. Note the local side stepping geometry and the occurrence of decimetre to metre scale mud-clasts. d) Close up view of mud-clasts contained in the previous dike. e) Cm-scale mud-clasts contained in a tar saturated dike at Bonny Doon Beach. Note the clast orientation probably acquired during emplacement of the sandstone intrusion. f) Rose diagram showing dike orientations in the Santa Cruz coastal area. Preferential N-S, WSW-ENE and SW-NE trends are evident.

Fig. 4. Main characteristics of sills and saucer-shaped intrusions forming the SCIC. a) Photograph and interpretative line drawing (b) of a sill cropping out at Panther Beach characterized by a marked upper erosional boundary. Internal structures are clearly visible and are mostly represented by plane-parallel banding. Note also arrays of near-vertical fractures cross-cutting the sandstone body. c) Photograph and interpretative line drawing (d) of nested tar-saturated saucer-shaped intrusions recognised at different stratigraphic levels in the Santa Cruz mudstone at 4 Mile Beach. e) Photograph and interpretative line drawing (f) of cross-section of a conical sandstone intrusion cropping out at 4 Mile Beach. Note that this sandstone body is connected with the underlying sandstone intrusion through a dike forming a cuspidate-shaped geometry.

Fig. 5. Main characteristics of sandstone-filled faults forming the SCIC. a) Photograph and interpretative line drawing (b) of a conjugate set of N-S and NNW-SSE faults recognised at Bonny Doon. The amount of offset, up to 15 cm, is provided by a dark marker clay level. c) Photograph and interpretative line drawing (d) of sandstone-filled normal fault recognised at Laguna Creek Beach. e) Photograph and interpretative line drawing (f) of detail from the previous outcrop. Note the complex structure of the fault plane and the sandstone intruded within even thin fault segments.

Fig. 6. Main characteristics of extrudites forming the SCIC at Red, White and Blue Beach. a) Photograph and interpretative line drawing (b) of bed-parallel, mound-shaped sand volcano displaying cross-bedding and isolated mud-clasts ripped up from the host strata. Note the underlying vent feeding the extrudite. The dark colour of the sandstone is attributable to the occurrence of tar.

Fig. 7. a) Photograph and interpretative line drawing (b) of NW-SE trending open fold deforming the Santa Cruz Mudstone at 4 Mile Beach. Note that the recent fluvial incision closely corresponds with the fold hinge zone where outer arc extension fracturing took place. c) Lower hemisphere equal area stereographic projection showing the orientation of the fault limbs and the resulting axial planes (great circles).

Fig. 8. a) Preferential orientations of faults recognised along the Santa Cruz coastal area. Note that faults shown on stereoplots are dominantly NNW-SSE and N-S trending. b) Conjugate normal faults forming a NNW-SSE trending graben in 4 Mile Beach. The measured amount of the offset, about 20 cm, is based on the displacement of dark marker beds alternating to the Santa Cruz Mudstone. c) Lower hemisphere equal area stereographic projections showing the orientation of the normal fault planes (great circles) in some key outcrops recognised along the investigated area. d) Normal fault showing smeared clay along the fault surface at Bonny Doon Beach. e) Striated strike slip fault exploiting a pre-existent discontinuity represented by the boundary between a sandstone intrusion and the Santa Cruz Mudstone at 4 Mile Beach. f) Lower hemisphere equal area stereographic projections showing the orientation of strike-slip faults (great circles) in some key outcrops recognised along the investigated area. g) Reverse faults recognised at 4 Mile Beach. Note the occurrence of tar-saturated injected sandstone within dilational jogs occurring along the fault plane. h) Line drawing interpretation.

Fig. 9. a) Details of the fracture network affecting the Santa Cruz Mudstone observable in plan view at 4 Mile Beach. b) S-shaped fractures and c) fracture meshes recognised at 4 Mile Beach. Note the occurrence of calcite within the fractures. d) Tar-saturated fracture recognised at 4 Mile Beach. e) Calcite-filled, *en-echelon* fractures at 4 Mile Beach. f) Lower hemisphere equal area stereographic projections showing the orientation of fractures (great circles) at 4 Mile Beach. g) Sets of conjugate fractures cutting through sandstone intrusions at Panther Beach. Note the resulting rhombohedral structure. h) Lower hemisphere equal area stereographic projections showing the orientation of fractures (great circles) at Panther Beach.

Fig. 10. a) Diagram showing the main range of trends of the tectonic structures recognised in the Santa Cruz Coastal area. The trends of the San Andres and San Gregorio fault zones are also included (red dotted lines). b) Diagram showing the main relationships between dike orientations (rose diagram) and fault and fracture patterns. Note that most dikes have been emplaced along extensional structures.

Fig. 11. Evidence for tectonic overprint of sandstone intrusions along the Santa Cruz coastal area. a) Photograph and interpretative line drawing (b) of 10 cm-thick sills overprinted by fractures recognised at 4 Mile Beach. Observable mechanical discontinuities mainly consist of fractures nearly orthogonal to the sill-host mudstone interface and bedding surfaces. Sill-parallel fractures are notably lacking. c) Sketch map of Shark Fin Cove with the sandstone intrusion shown in red. d) Portion of the considered sandstone intrusion scarcely affected by later tectonic deformation. Conjugate fractures are visible in the host strata but, importantly, do not affect the dike-host-strata interface. e) Same dike in a sector characterized by strong post-emplacement deformation probably related to a normal fault zone. The deformed dike shows steps and thickened sections due to vertical compression. f) Most of the deformation is focussed along the dike-host-strata interface where a thick unit of cataclastic material forms. g) Photograph and interpretative line

drawing (h) of a dike affected by post emplacement deformation recognised at Laguna Creek Beach. Similar to the previous example, vertical compression is accommodated by conjugate fractures, stepped geometry and thickening in the central portion of the dike.

Fig. 12. a) Photograph and interpretative line drawing (b) of cross-cutting relationships between the two recognised generations of sandstone intrusions at Panther Beach. c) Lower hemisphere equal area stereographic projections (great circles) showing the orientation of the conjugate sandstone-filled normal faults recognised at Panther Beach. d) Fault 1 shows a cm-scale offset and is only partially filled by sand. e) Close-up of Fault 1 showing the younger generation of sandstone intrusions emplaced along the fault plane, and the low-angle dike belonging to the older generation that is fractured and thinned in the proximity of the fault plane. f) Line drawing interpretation showing fracture distribution along the low-angle dike with respect to the distance from the fault plane. g) Photograph of Fault 2. h) *En echelon* dilation fractures partially filled by fluidised sand recognised along the Fault 2. i) Line drawing interpretation. k) Photograph and l) interpretation of Fault 3.

Fig. 13. Evolutionary model proposed to explain the occurrence of the Santa Cruz Injection Complex and the Santa Cruz petroleum system. a) The Santa Cruz Injection Complex emplacement mainly occurred during the Late Miocene following a contractional deformation stage affecting the Santa Cruz sedimentary succession. Sand remobilization and emplacement related to the first sand injection event was particularly intense in the correspondence of the anticlines where fluid overpressure generated by the squeezing of the Santa margarita Sandstone and fracturing promoted by outer arc extension created suitable conditions. The age of the sandstone intrusion event is constrained to the Late Miocene by the extrudites recognised in the study area. b) The unconsolidated state of the Santa Cruz Mudstone and the successive accumulation of sediments at the top of the sandstone intrusion complex caused the resealing of the system and favoured the accumulation of hydrocarbons pertaining to Santa Cruz petroleum system in the newly-formed

908 sandstone network between the Late Miocene and the Early Pliocene. c) Uplift and faulting (with
909 the formation of sandstone-filled faults) related to the Pliocene-Quaternary strike-slip tectonic
910 evolution of the area caused the definitive failure of the Santa Cruz petroleum system. Tar-
911 saturated sandstones are what remain of this petroleum system.

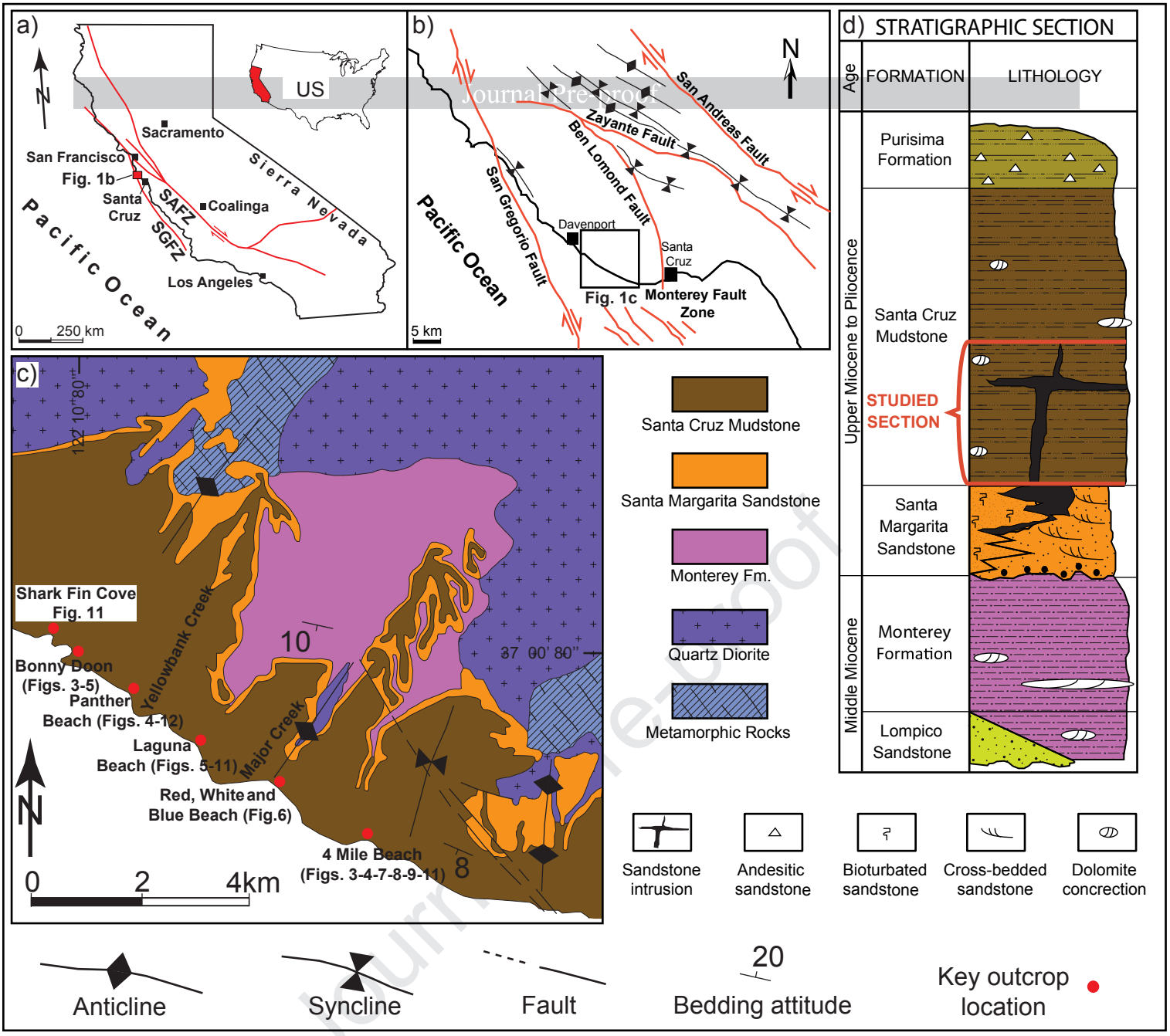

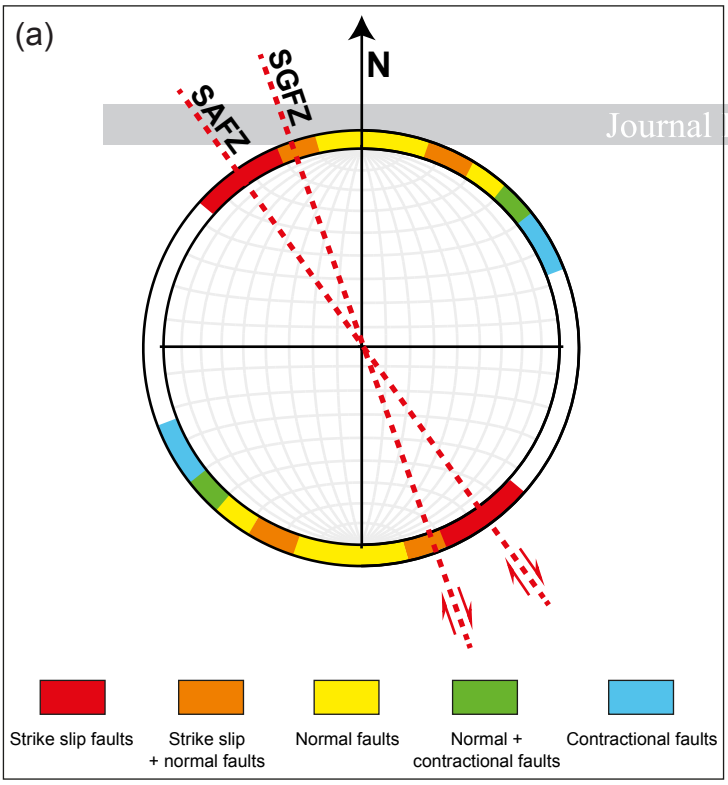

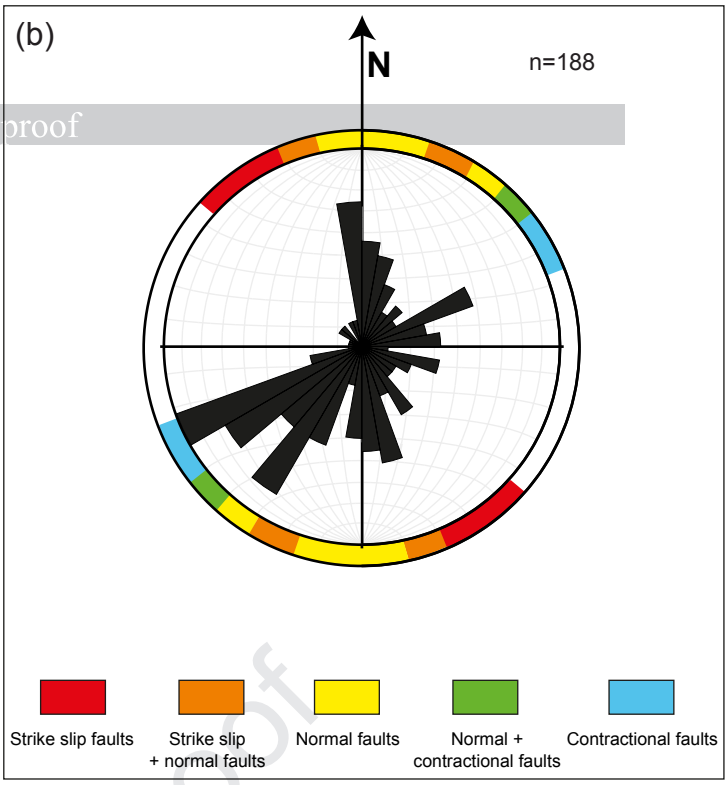

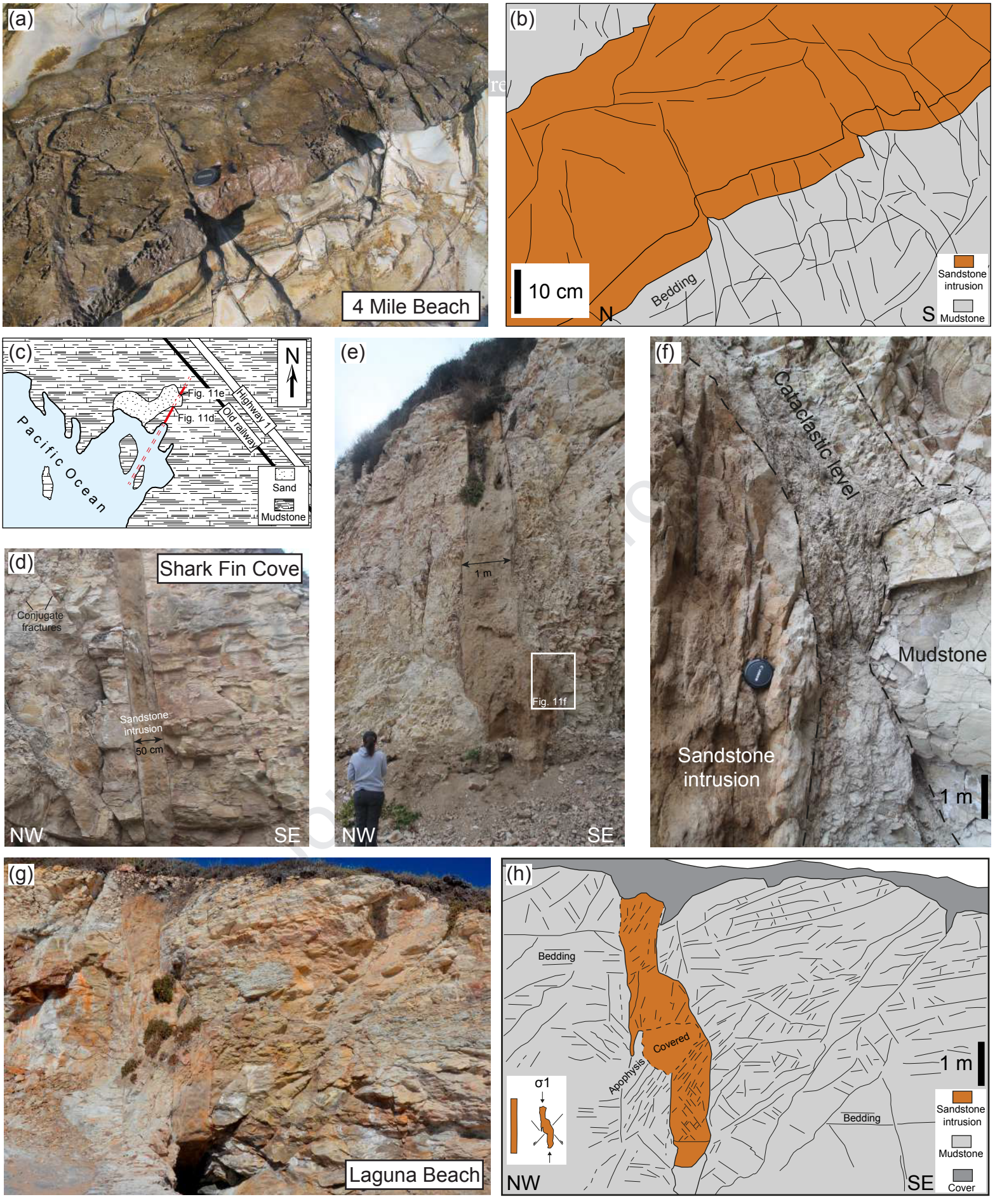
(a)
4 Mile Beach
(b)
10 cm
N
Bedding
S
Sandstone intrusion
Mudstone
(c)
N
Fig. 11e
Fig. 11d
Highway 1
Old railway
Pacific Ocean
Sand
Mudstone
(d)
Shark Fin Cove
Conjugate fractures
Sandstone intrusion
50 cm
NW
SE
(e)
1 m
Fig. 11f
NW
SE
(f)
Cataclastic level
Mudstone
Sandstone intrusion
1 m
(g)
Laguna Beach
(h)
Bedding
Covered
Apophysis
σ1
1 m
Bedding
Sandstone intrusion
Mudstone
Cover
NW
SE

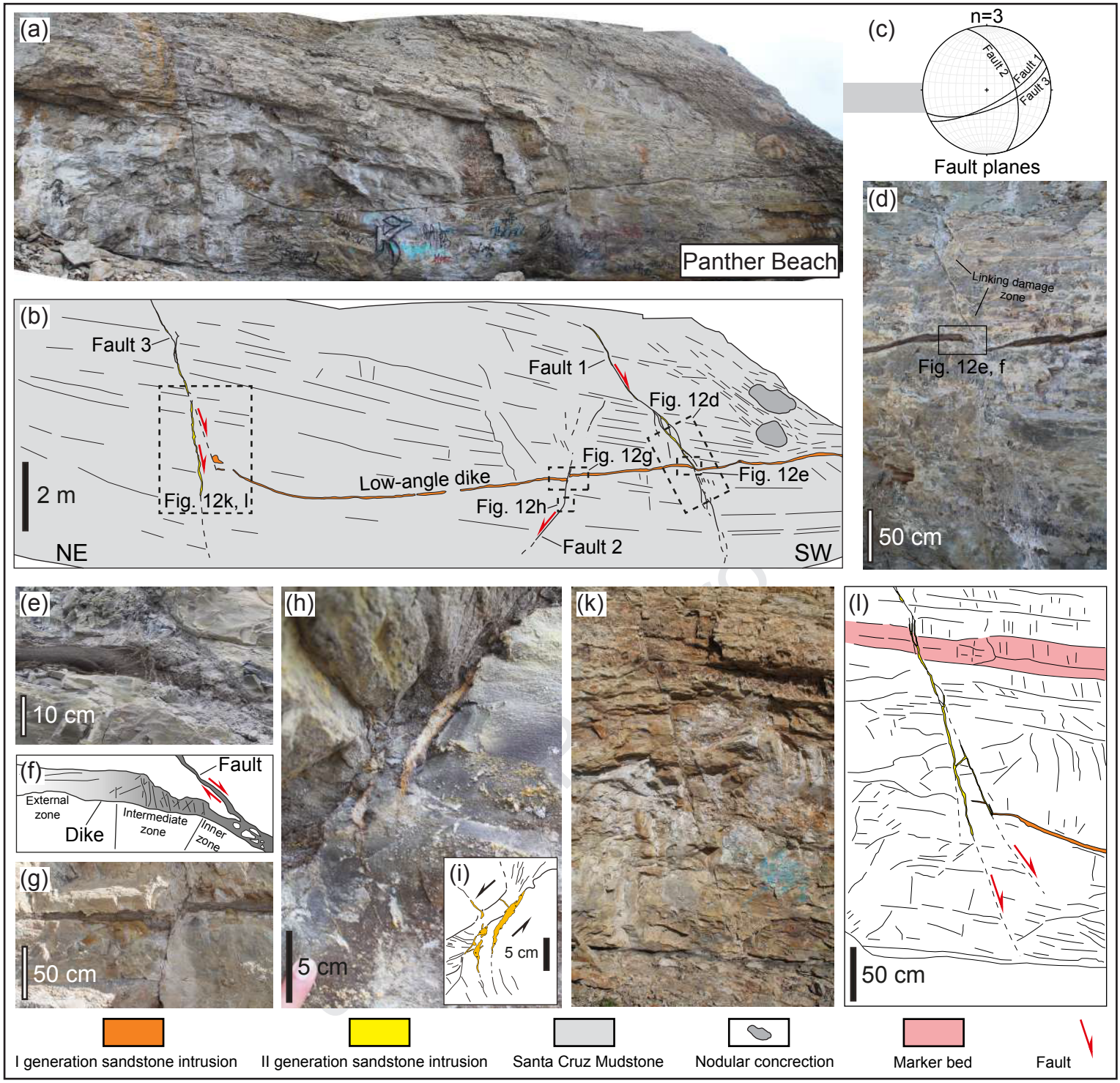
(a)
Panther Beach
(b)
Fault 3
Fault 1
Fig. 12d
Fig. 12g
Fig. 12e
Low-angle dike
Fig. 12h
Fig. 12k, l
Fault 2
2 m
NE
SW
(c)
n=3
Fault 1
Fault 2
Fault 3
Fault planes
(d)
Linking damage zone
Fig. 12e, f
50 cm
(e)
10 cm
(f)
Fault
External zone
Dike
Intermediate zone
Inner zone
(g)
50 cm
(h)
5 cm
(i)
5 cm
(k)
(l)
50 cm
I generation sandstone intrusion
II generation sandstone intrusion
Santa Cruz Mudstone
Nodular concrection
Marker bed
Fault

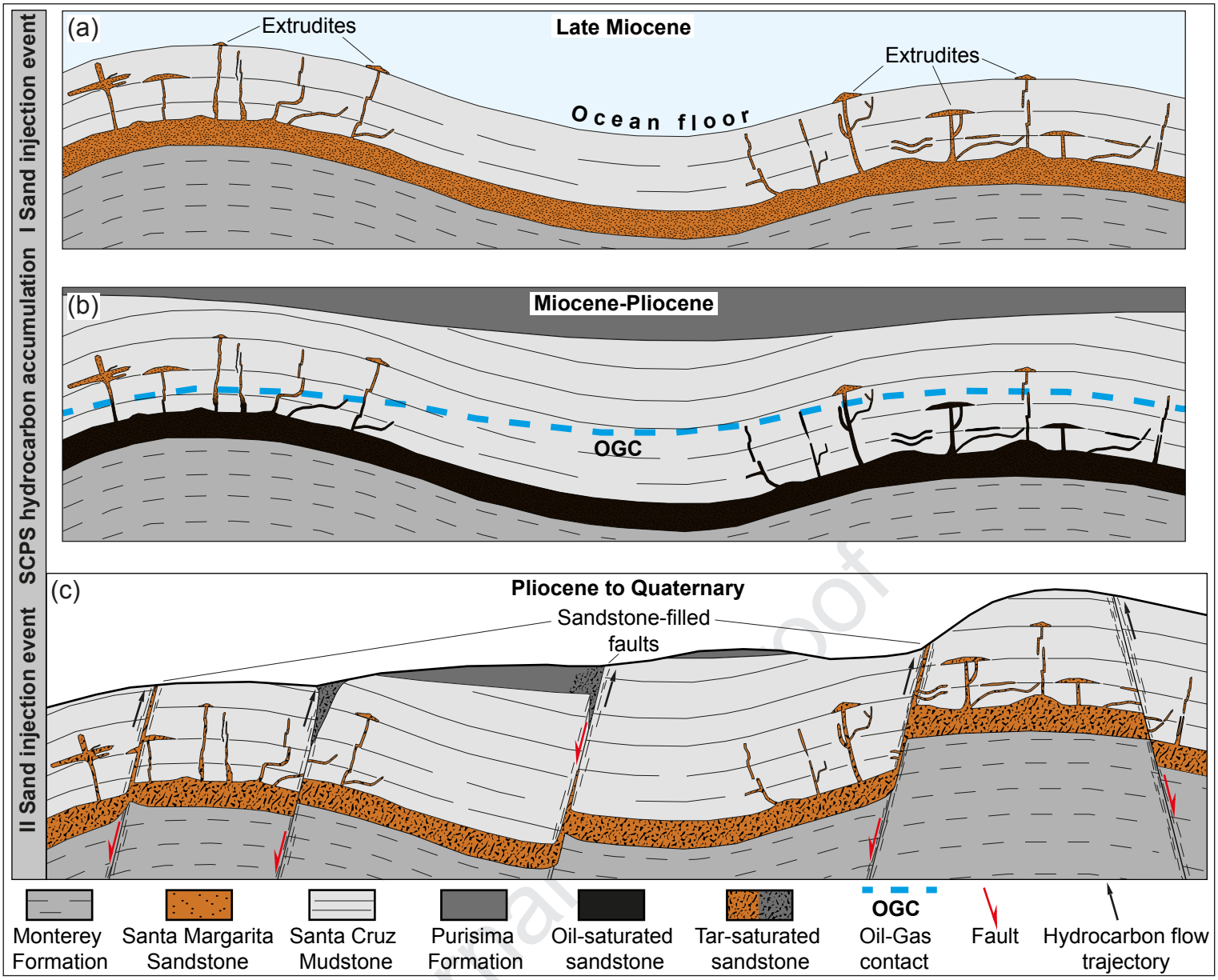

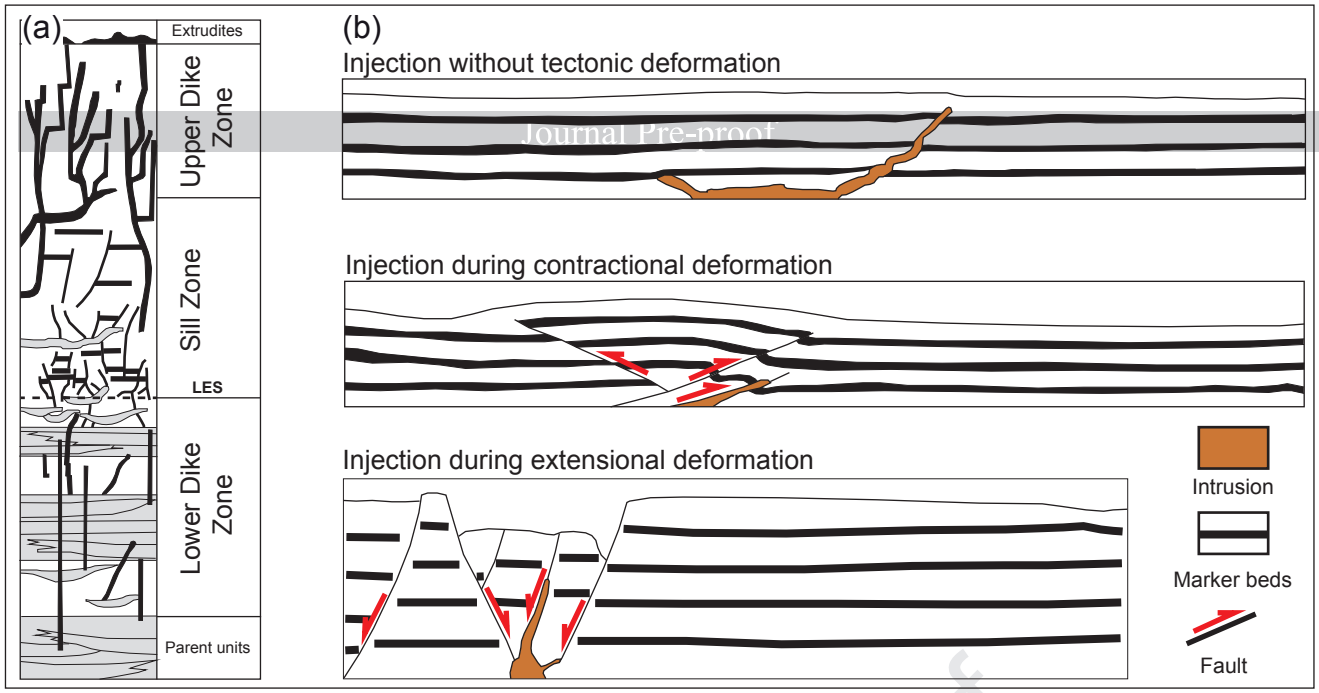

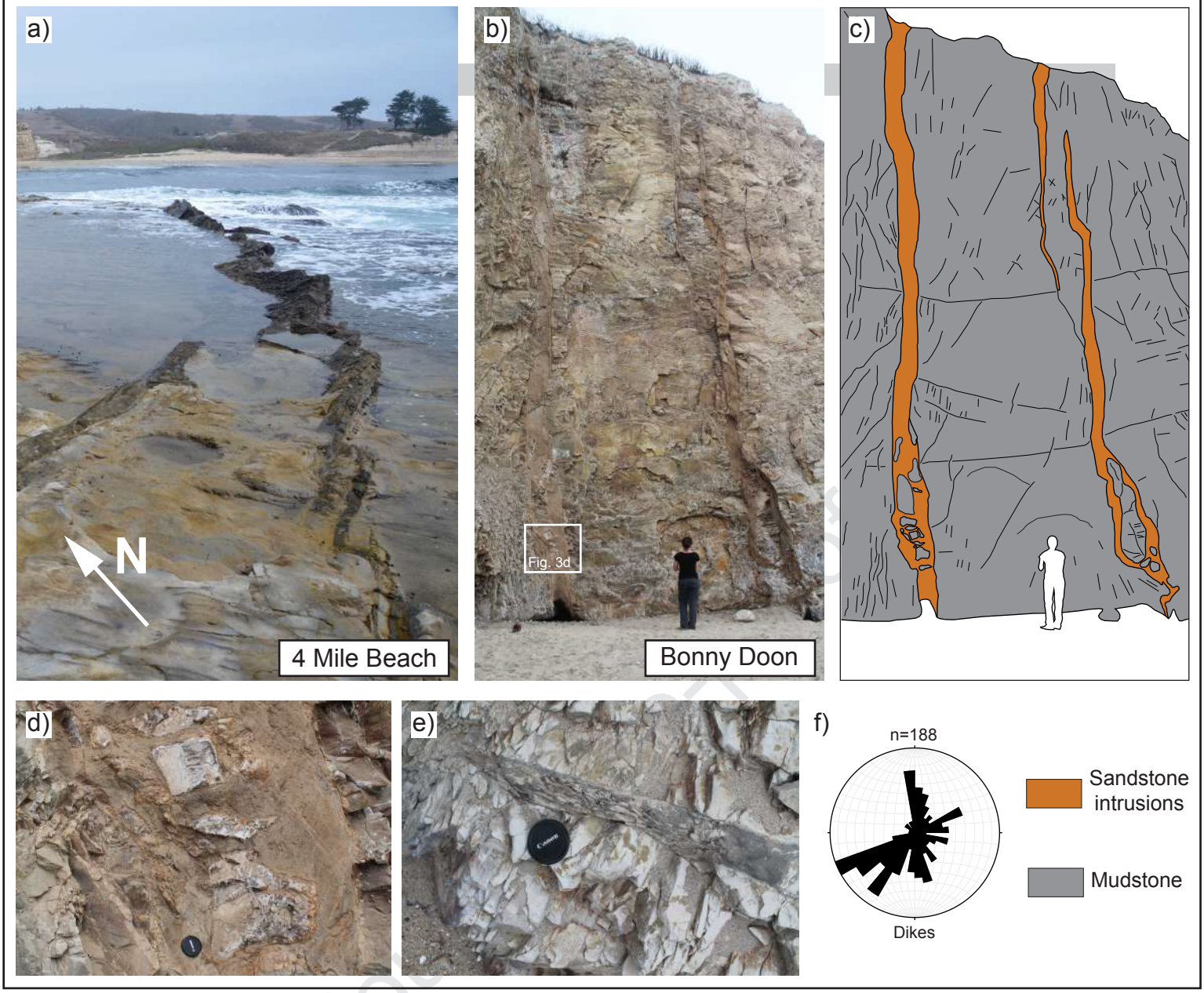
a)
N
4 Mile Beach
b)
Fig. 3d
Bonny Doon
c)
d)
e)
f)
n=188
Dikes
Sandstone intrusions
Mudstone

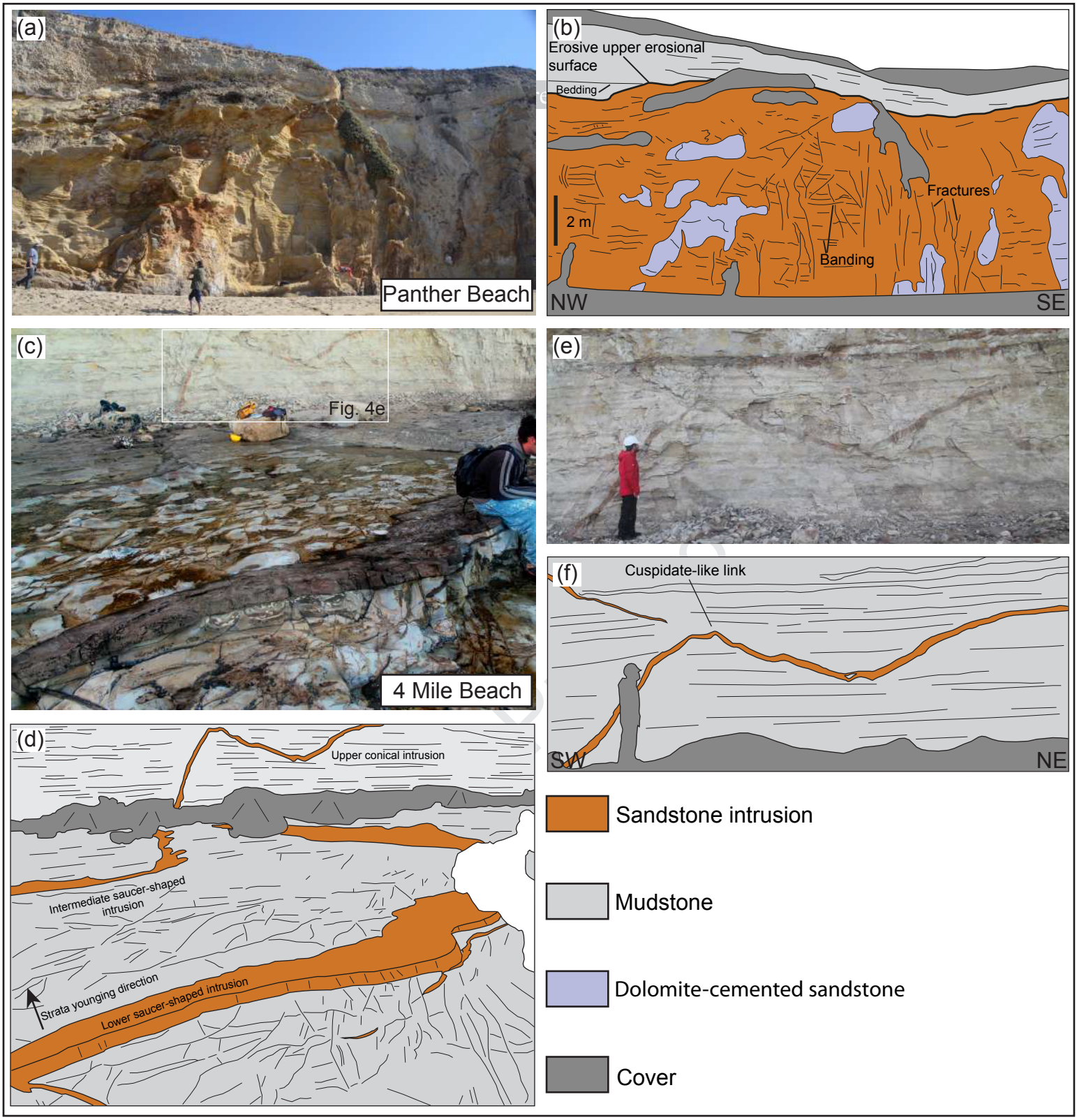
(a)
Panther Beach
(b)
Erosive upper erosional surface
Bedding
2 m
Fractures
Banding
NW
SE
(c)
Fig. 4e
4 Mile Beach
(e)
(f)
Cuspidate-like link
SW
NE
(d)
Upper conical intrusion
Intermediate saucer-shaped intrusion
Strata younging direction
Lower saucer-shaped intrusion
Sandstone intrusion
Mudstone
Dolomite-cemented sandstone
Cover

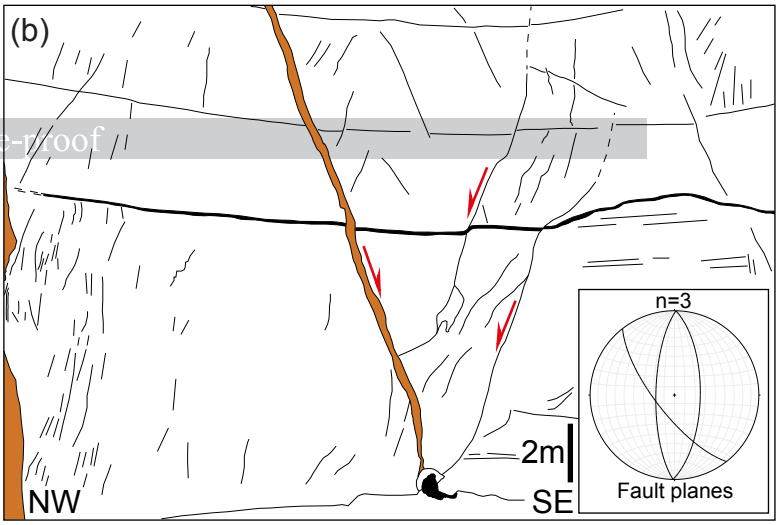

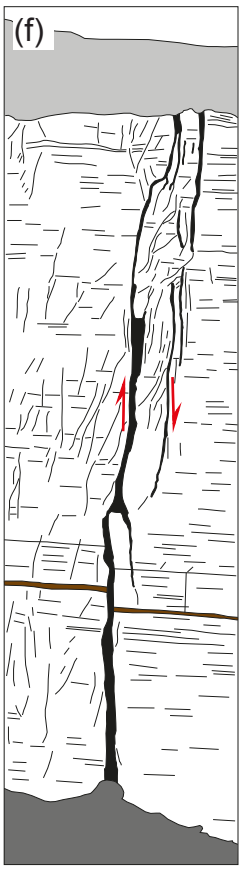

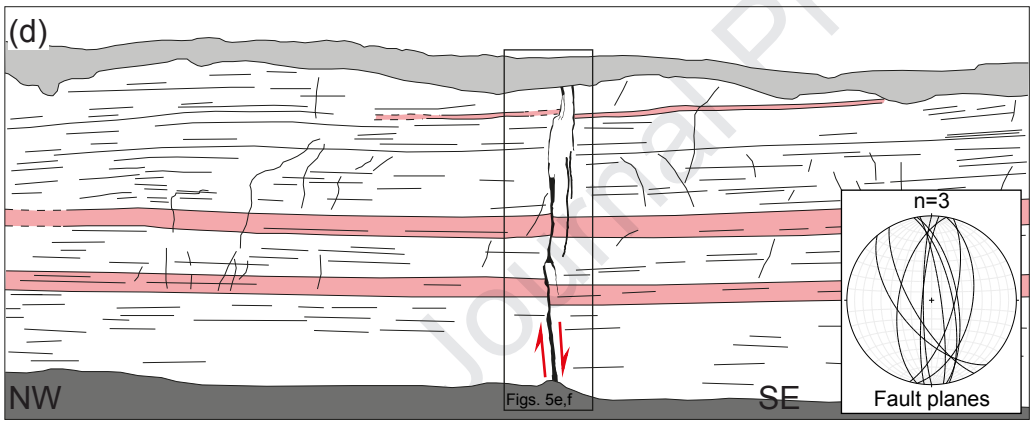

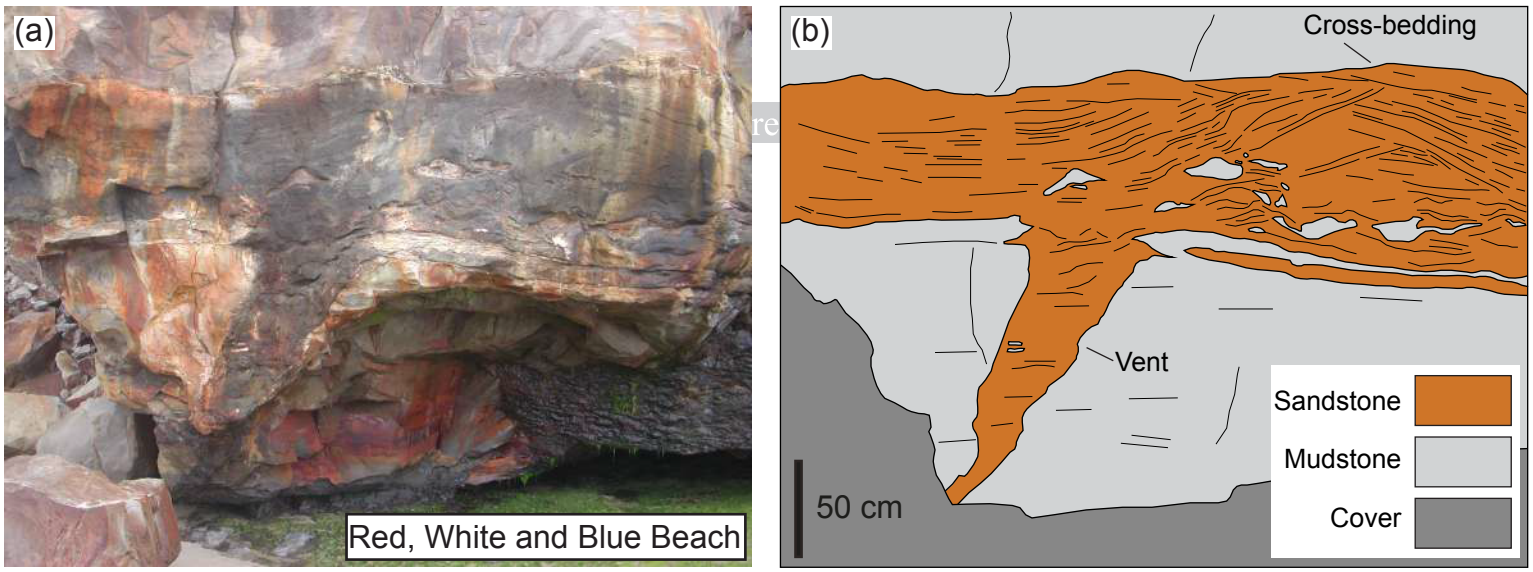

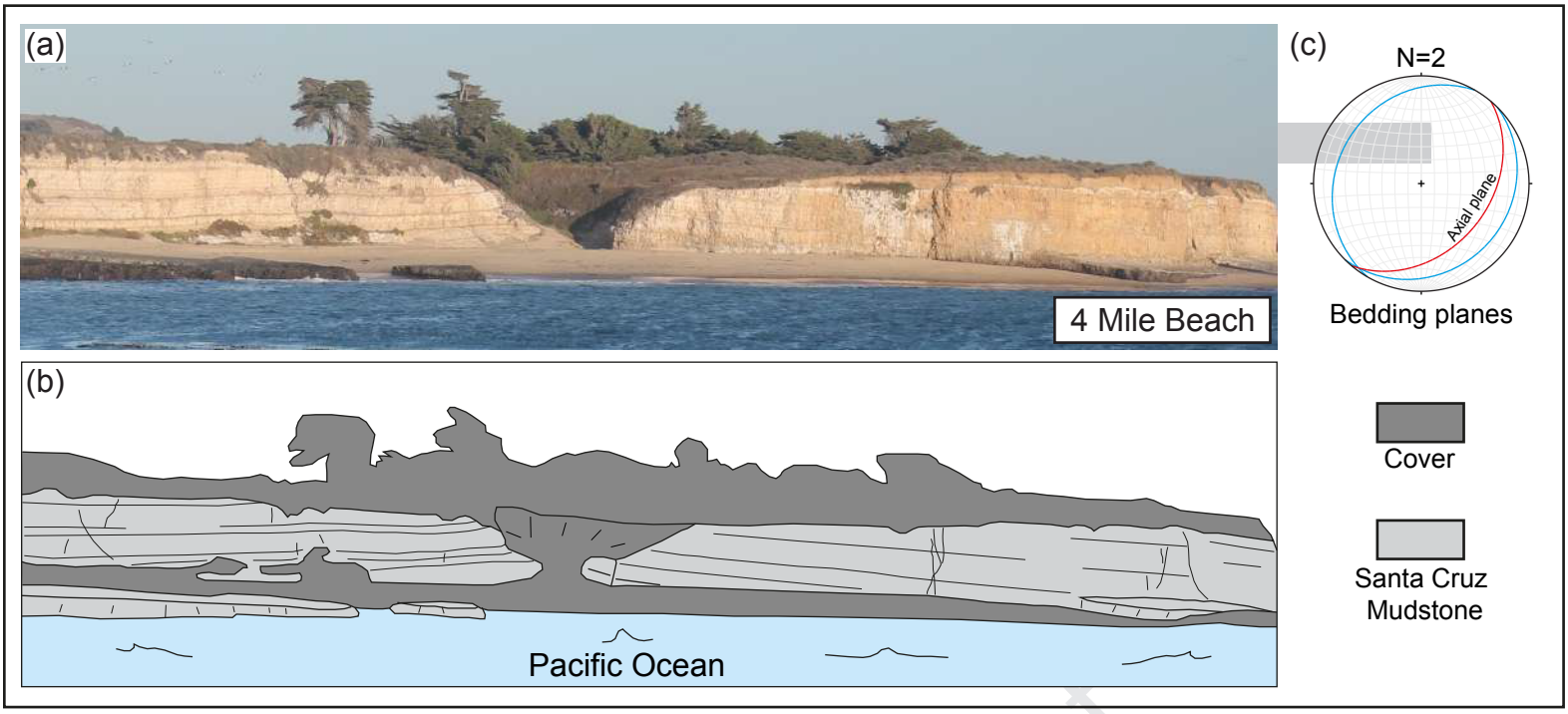

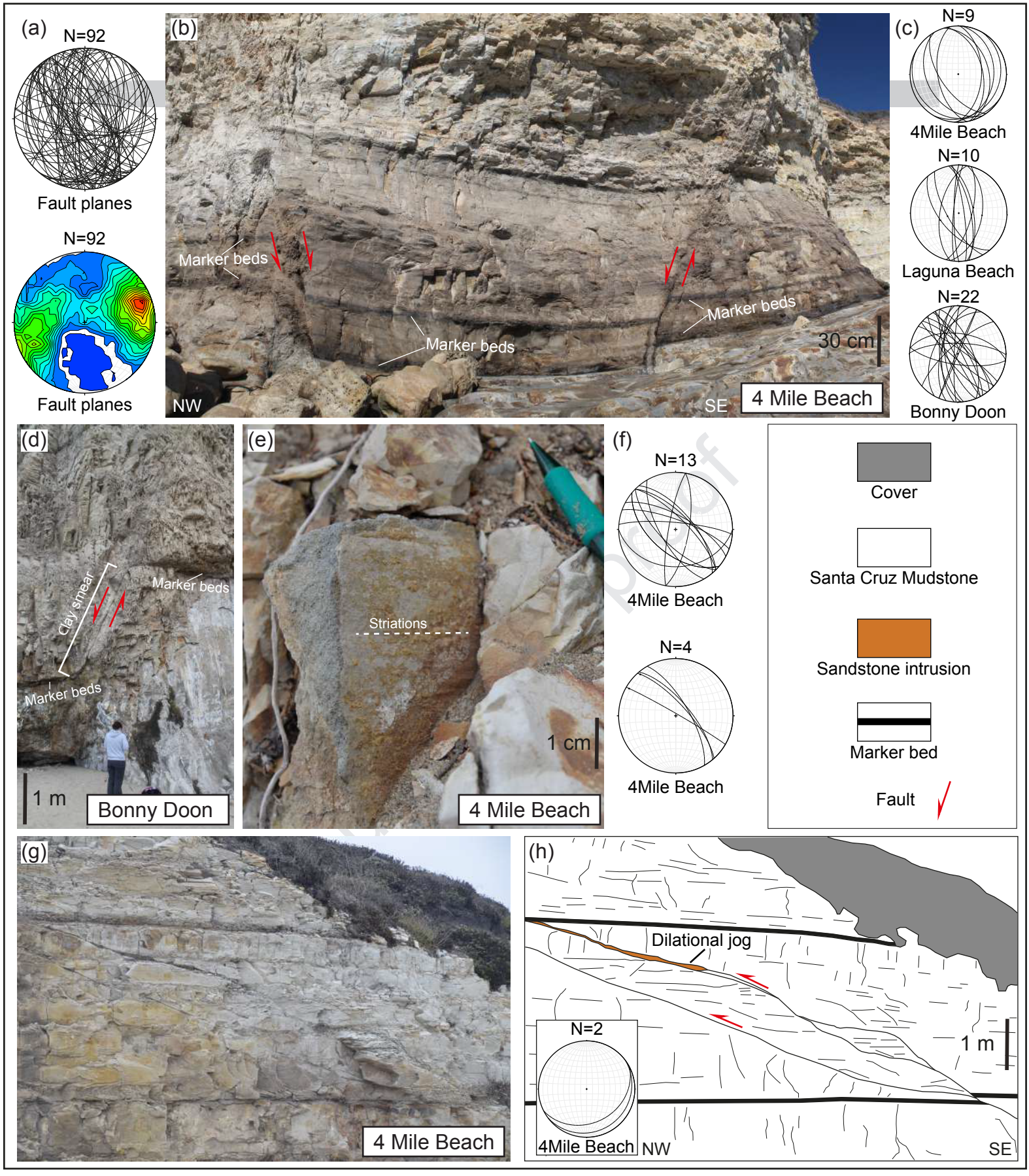
(a)
N=92
Fault planes
N=92
Fault planes
(b)
Marker beds
Marker beds
Marker beds
30 cm
NW
SE
4 Mile Beach
(c)
N=9
4Mile Beach
N=10
Laguna Beach
N=22
Bonny Doon
(d)
Clay smear
Marker beds
Marker beds
1 m
Bonny Doon
(e)
Striations
1 cm
4 Mile Beach
(f)
N=13
4Mile Beach
N=4
4Mile Beach
Cover
Santa Cruz Mudstone
Sandstone intrusion
Marker bed
Fault
(g)
4 Mile Beach
(h)
Dilational jog
N=2
4Mile Beach
NW
SE
1 m


(a)


(b)


(c)


(d)


(e)

(f)

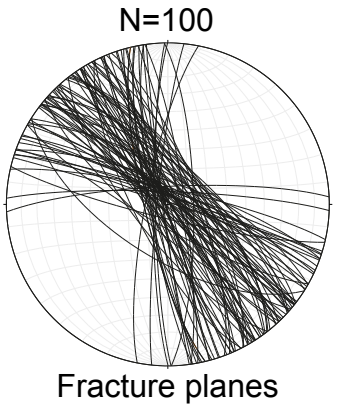
N=100
Fracture planes


(g)

(h)

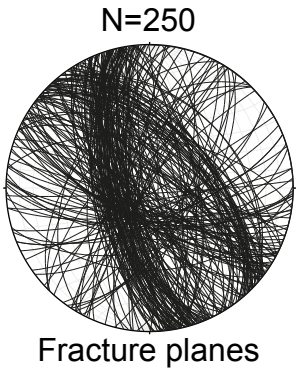
N=250
Fracture planes

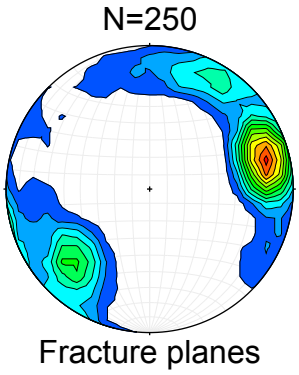
N=250
Fracture planes

- Evolution of the Santa Cruz petroleum system was accompanied by sandstone intrusion.
- Sandstone-filled faults are consistent with tectonics of the San Andreas Fault.
- Hydrocarbon leakage occurred through fractures and sandstone-filled faults.

The authors declare that there is no conflict of interest.